THE JOURNAL
OF
CHEMICAL PHYSICS

VOLUME 6 APRIL, 1938 NUMBER 4

The Mercury Photosensitized Decomposition of Ethane*

E. W. R. STEACIE AND N. W. F. PHILLIPS
Physical Chemistry Laboratory, McGill University, Montreal, Canada

(Received January 10, 1938)

An investigation of the mercury photosensitized decomposition of ethane has been made, the products of the reaction being analyzed by low temperature fractional distillation. It is found that by improved trapping methods it is possible to remove butane from the system as formed, and thus the formation of secondary products is entirely inhibited. Under these circumstances the products of the reaction consist exclusively of methane, propane, and butane, the hydrogen and higher hydrocarbons found in previous investigations being secondary products of the propane and butane decompositions. The quantum yield (in terms of ethane disappearing) is approximately 0.2. The suggested mechanism of the reaction is:

$$C_2H_6+Hg(2^3P_1)=2CH_3+Hg(1^1S_0)$$
$$CH_3+C_2H_6=CH_4+C_2H_5$$
$$2CH_3=C_2H_6$$
$$2C_2H_5=C_4H_{10}$$
$$CH_3+C_2H_5=C_3H_8.$$

INTRODUCTION

A GREAT many papers have been published on the decomposition reactions of the simple hydrocarbons, thermal, photochemical, photosensitized, free radical sensitized, etc.[1] The mercury photosensitization method has certain marked advantages, since the input of energy to the reactant molecule is a very definite process. With the development of improved light sources and analytical methods it has become possible to obtain much more detailed and definite information, and a re-investigation of the photosensitized decomposition reactions of the simple paraffins has therefore been commenced in this laboratory.

The present paper deals with the mercury photosensitized decomposition of ethane. This reaction was first studied by Taylor and his collaborators in the course of their classical investigations of mercury photosensitized reactions. Taylor and Hill[2] observed that in ethylene-hydrogen mixtures ethane and higher hydrocarbons were formed. After the pressure change accompanying this reaction was over, other changes occurred which led them to suspect that the ethane formed was being attacked both by hydrogen atoms and by excited mercury. They verified this, and suggested that radicals were undoubtedly involved in the process.

Kemula[3] also showed that ethane could be decomposed by excited mercury atoms. A more thorough investigation of the reaction was made by Kemula, Mrazek and Tolloczko[4] following on earlier work by Tolloczko.[5] In their investigation the reaction mixture was circulated through a trap at −80°C to remove the products

* The work described in this paper was done with financial assistance from the National Research Council of Canada, which is hereby gratefully acknowledged.

[1] See Steacie, Chem. Revs. April (1938) for references.

[2] Taylor and Hill, J. Am. Chem. Soc. **51**, 2922 (1929).

[3] Rocz. Chem. **10**, 273 (1930).

[4] Kemula, Mrazek and Tolloczko, Coll. Czech. Chem. Comm. **5**, 263 (1933).

[5] Tolloczko, Przemysl Chem. **11**, 245 (1927).

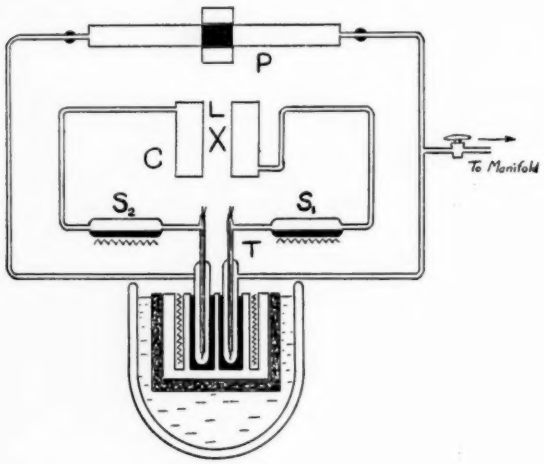

FIG. 1.

of higher molecular weight as fast as formed, and thus prevent secondary processes. (This is not a sufficiently low temperature to remove butane efficiently, since its vapor pressure is 11 mm at −80°C, and the prevention of secondary changes was thus only partially successful.) They found that the decrease in pressure as the reaction progressed was accompanied by an exactly parallel increase in the volume of the liquid condensate. The rate was independent of the ethane pressure, but at high pressures a higher percentage of condensate was formed. The gaseous products consisted entirely of hydrogen and methane, the ratio of hydrogen to methane being considerably greater than unity, and approaching infinity if the trap were kept at −20°C instead of −80°C. The condensable products were analyzed by a rough fractional distillation, and were found to consist mainly of butane and octane, with a small amount of hexane and no propane or pentane.

Tolloczko had previously suggested that the mechanism of the process was

$$2C_2H_6=2C_2H_5+2H=C_4H_{10}+H_2,$$
$$C_2H_6+C_4H_{10}=C_2H_5+C_4H_9+2H$$
$$=C_6H_{14}+H_2, \text{ etc.}$$

This assumes only a C−H rupture and leads obviously to hydrocarbons with an even number of carbon atoms only. It gives, however, no explanation of the formation of methane. Kemula, Mrazek and Tolloczko therefore suggested

$$C_2H_6+Hg(2^3P_1)=C_2H_6{}^*+Hg(1^1S_0),$$
$$C_2H_6{}^*=C_2H_5+H,$$
$$2C_2H_5+M=C_4H_{10}+M,$$
$$2H+M=H_2+M,$$
$$C_2H_6+H=C_2H_5+H_2,$$
$$C_2H_6+H=CH_3+CH_4.$$

The higher hydrocarbons then result from secondary reactions of butane, etc. The fact that octane is the main higher product suggests that the chief reaction of butane is

$$Hg(2^3P_1)+C_4H_{10}=C_4H_9+H+Hg(1^1S_0),$$
$$2C_4H_9+M=C_8H_{18}+M.$$

As we shall see, however, the efficient removal of butane from the system causes a pronounced change in the products of the reaction.

EXPERIMENTAL

Apparatus and procedure

A dynamic method was employed. The apparatus is shown diagrammatically in Fig. 1.

The light source L was a Hanovia Sc2537 mercury resonance lamp. The lamp was in the form of a double U, and was run at 100 milliamperes with a 5000-volt sign transformer. (The actual potential across the lamp after it had warmed up was about 370 volts.) The radiation from the lamp was used directly without filtering, since blank experiments showed that no reaction occurred when ethane was illuminated in the absence of mercury. The fused quartz reaction vessel C was annular in form, being 10 cm long, 8 cm in diameter, with a hole 4 cm in diameter through the middle. Its volume was 320 cc. A well in the side of the vessel was provided to accommodate a thermocouple.

The pump P consisted of a brass tube 40 cm long and 4 cm diameter inside which was a close-fitting steel cylinder. A solenoid of about 1000 ampere-turns was arranged to slide on the outside of the tube, and a reciprocating motion was applied to the solenoid by means of a wheel and crank. The displacement of the pump was 350 cc, so that the entire contents of the reaction vessel were displaced each half-cycle.

The saturation of the gas with mercury vapor

was accomplished by means of the vessels S_1 and S_2, each of which provided a mercury surface of about 30 cm². The saturators were heated electrically to about 60°C.

As mentioned above, one of the main objects of the present work was the elimination of secondary processes by the removal of hydrocarbons of higher molecular weight from the system as fast as formed. With this end in view the gases were circulated through the traps T. The method by which these traps were maintained at definite low temperatures for long periods of time was as follows. The traps were immersed in mercury contained in two holes drilled in a steel block. Small electric heaters were inserted in other holes in the same block. The block was surrounded by an insulating layer of cotton encased in a sheet metal container, and the container was immersed in liquid oxygen. By keeping the liquid oxygen level constant and varying the electrical input, it was possible to maintain the traps at any desired temperature in the range to be studied. The temperature could thus be controlled to within 1–2°. The temperature of the traps was measured by means of copper-constantan thermocouples situated inside the traps themselves. These were calibrated at the boiling points of oxygen and ethylene, at the sublimation point of carbon dioxide, and from −50° to 0°C by means of standard thermometers.

The main portion of the apparatus had a total volume of about 1200 cc. It was connected to a manifold which led to the pumping system, a McLeod gauge, gas reservoirs, a Toepler pump, gas holders, etc.

In later runs mercury valves were used so that circulation occurred in the same direction during both strokes of the pump, and only one trap and saturator were used. The total volume of the altered system was 1500 cc. No changes in the optical system were made.

In making a run, a suitable amount of gas was introduced into the reaction system, and the traps T were brought to the desired temperature. The pump P was started, and the saturators were heated to 60°C. The gas was then illuminated for a definite period of time. At the conclusion of this period, the traps were brought to room temperature and the products of reaction were completely pumped by the Toepler pump into a portable gas holder. The gas was then analyzed by low temperature fractional distillation in an apparatus of the Podbielniak type. A 500 cc sample could thus be analyzed for the gaseous constituents (i.e., those with boiling points below room temperature) with an accuracy of about 0.5 percent. In the analysis methane and hydrogen were taken off together, and this fraction was analyzed by combustion in the usual way. The distillation apparatus available was not suitable for the analysis of high boiling products. However, as will be shown later, such products were only present when secondary reactions occurred, and were entirely absent during the more significant experiments.

Materials

Ethane and butane were obtained in cylinders from the Ohio Chemical and Manufacturing Company. The gases were stated to be not less than 97 and 99 percent pure, respectively. Analysis of the cylinder ethane showed it to contain 1.3 percent ethylene, less than 0.3 percent of H_2+CH_4, and less than 0.3 percent of higher hydrocarbons. This gas was passed over hot copper oxide, through a 40 percent KOH solution and a trap at −80°C, and was then condensed and fractionally distilled. Butane was purified merely by fractional distillation. Hydrogen was taken from cylinders and passed over platinized asbestos at 600°C, and then through a liquid-air trap.

TABLE I. *Absorption of the resonance line under various conditions. Arc current, 0.100 amp. Cell temperature, 35°C. Mercury saturation at 35°C=4×10⁻³ mm.*

Foreign Gas	Pressure, mm	Resonance Radiation Absorbed, erg cm⁻³	Fraction of Resonance Radiation Absorbed
H_2	180	8.0×10^{15}	1.00
	87	7.7	0.96
	72	7.6	0.95
	51	7.4	0.92
	10	5.2	0.65
C_2H_6	680	7.8×10^{15}	0.97
	420	7.8	0.97
	330	7.8	0.97
	210	7.7	0.96
	171	7.7	0.96
	151	7.6	0.95
	136	7.5	0.94
	75	7.0	0.87
	40	6.3	0.79
	10	4.3	0.54

TABLE II. *The mercury photosensitized decomposition of ethane. Volume of system = 1200 cc (1500 cc in runs 7 and 8). Resonance radiation absorbed = 4.0×10^{-6} einsteins per sec. Volume of cell = 320 cc. Cell temperature = 35°C. Arc current = 0.100 amp. Arc voltage = 370. Mercury vapor pressure = 4×10^{-3} mm.*

Run No.	Time, hr.	Initial Pressure, cm	Final Pressure, cm	Trap Temperature, °C	Circulation Rate, Liters per min.	Partial Pressure of C_2H_6 During Run	Fraction of C_2H_6 Decomposed	Decomposition Rate, Mole per sec. $\times10^6$	Quantum Yield (ethane reacting)	Products, Mole Percent				
										H_2	CH_4	C_3H_8	C_4H_{10}	Higher Hydrocarbons (as C_8)
1	10	44.1	42.0	− 70	6	40 to 15	0.67	0.53	0.13	47	16	none	23	14
2	8	43.1	41.8	− 70	6	40 to 15	0.60	0.58	0.14	43	23	none	20	14
3	8.5	42.2	41.9	−100	1.3	40 to 20	0.50	0.44	0.11	—	—	—	25	present
4	8	75.0	75.0	−108	1.2	25	0.23	0.38	0.095	19.6	44.7	none	35.7	trace
5	15	73.2	73.2	−115	4	15	0.45	0.39	0.098	—	—	—	—	none
6	20	69.9	69.9	−116	6	15	0.58	0.36	0.090	6.1	59.3	<1.0	34.6	none
7	8.75	39.0	39.0	−125	3	7	0.55	0.54	0.15[a]	0.0	59.5	21.5	19.0	none
8	6.75	39.0	39.0	−131	3	4	0.45	0.61	0.18[b]	0.0	58.8	23.5	17.7	none

[a] The ethane partial pressure was too low for complete absorption of the incident resonance radiation. Hence in this run the absorbed resonance radiation was only 3.7×10^{-6} einsteins per sec.
[b] Resonance radiation absorbed = 3.4×10^{-6} einsteins per sec.

The intensity of the light source

The intensity of the mercury resonance radiation was determined by measuring the rate of hydrolysis of monochloroacetic acid.[6] Two concentrations of the acid were employed, 0.5*N* and 0.25*N*. These gave identical results, showing that absorption was complete. The solution after irradiation was neutralized with $NaHCO_3$ and titrated with $AgNO_3$, using K_2CrO_4 as an indicator. The mean of a number of concordant measurements made at different times gave for the total resonance radiation entering the cell 4.2×10^{-6} einsteins per second.

The light intensity was also measured by means of a Moll thermopile in conjunction with a galvanometer. The thermopile was placed outside the reaction vessel, and the intensity of resonance radiation was determined by taking the difference in thermopile readings with the cell evacuated, and with it filled with mercury vapor at 35°C in the presence of a high hydrogen pressure. This method gave a value of 3×10^{-6} einsteins per second. Considering the uncertainty in this method due to the geometry of the cell, etc., the agreement of this result with that obtained actinometrically is better than could be expected.

The absorption of resonance radiation

By means of the galvanometer-thermopile system, measurements were made of the absorption of resonance radiation by mercury vapor in the presence of ethane and hydrogen. During these experiments the gases were circulated over the mercury saturators as in a normal run, the mercury vapor pressure thus being maintained at approximately 4×10^{-3} mm. With this precaution the amount of absorbed resonance radiation became constant in less than one minute after admitting the gas to the system. Measurements were made rapidly in the case of ethane in order to avoid appreciable decomposition. The results of these measurements are given in Table I.

Measurements of the efficiency of the absorption were also made by observing the rate of the mercury photosensitized hydrogen-oxygen reaction in an auxiliary quartz cell placed close to the outside of the reaction cell. The ratio of the rates of combination of hydrogen and oxygen with the reaction cell empty, and with it filled with ethane at 650 mm pressure in the presence of mercury at its vapor pressure at 35°C was 40. This is an excellent check on the absorption at

TABLE III. *The mercury photosensitized decomposition of butane.*

Operating conditions	as in Table II
Time, hours	4.5
Initial pressure, cm	59.5
Final pressure, cm	40.25
Trap temperature, °C	0.0
Fraction decomposed	0.88
Hydrogen produced, cm	30.0
Mole decomposed per second	2.2×10^{-6}
Quantum yield	0.55
Mole hydrogen formed per second	1.3×10^{-6}

[6] Rudberg, Zeits. f. Physik **24**, 247 (1924).

high ethane pressures as determined by thermopile measurements.

Results

The results are given in Table II. One run was also made with butane, for reasons to be discussed later, and the data for this are given in Table III. Several runs were also made with $C_2H_6-H_2$ mixtures, the results of which are given in Table IV. The "initial" and "final" pressures given in columns 3 and 4 of Table II are those with the traps at room temperature before and after the run. The values of the initial partial pressure of ethane in column 7 are lower than the values in column 3 for the later runs, since the initial ethane pressure was higher than the vapor pressure of ethane at the trapping temperature, and some ethane condensed in the traps. Column 5 gives the temperature of the traps, and thus expresses qualitatively the degree of removal of high boiling products. In runs (4), (5), (6), (7), and (8) the vapor pressures of propane and butane should be less than those inferred from the temperature of the traps, because of their solubility in the condensed ethane in the traps. The vapor pressures of propane and butane at a few temperatures are given in Table V to show the extent to which they were removed at the various trapping temperatures employed. Still lower trapping temperatures were, of course, not feasible on account of the diminution in the vapor pressure of ethane.

It is apparent from the analytical data that the circulation rates employed were sufficiently high to insure complete absence of secondary decomposition products when sufficiently low trapping temperatures were employed.

As pointed out previously, the analytical apparatus available was not satisfactory for the determination of higher hydrocarbons. In runs in which such products were present, they are reported as C_8H_x, calculated from a carbon balance, since the boiling point of the residue corresponded with that of octane. Actually, the higher fraction was by no means pure octane, since it had an aromatic odor, and since qualitative tests showed the presence of some unsaturation. In the later, and more important runs, however, no higher hydrocarbons were present and the analyses are therefore complete. In these runs perfect material balances were obtained.

Before entering on a discussion of the mechanism of the reactions it will be convenient to summarize the main conclusions to be drawn from the data of Tables II, III, and IV.

(1) The decomposition of ethane

(a) At high trapping temperatures, in agreement with the results of previous investigators, much hydrogen is produced, the H_2/CH_4 ratio being approximately 3. Considerable butane and higher hydrocarbons are formed, but no propane.

(b) When the trapping temperature is reduced to about $-115°C$, the formation of higher hydrocarbons is entirely inhibited, and much butane is produced. At the same time the production of hydrogen decreases greatly, the H_2/CH_4 ratio falling to about $\frac{1}{3}$.

Table V.*

Temperature, °C	Vapor Pressures, mm Propane	Butane
− 70	209	19
−100	30	2
−110	13	0.7
−120	5	0.3
−130	2	0.07

* Values taken from *International Critical Tables*.

Table IV. *Experiments with added hydrogen. Volume of system = 1500 cc. Volume of cell = 320 cc. Cell temperature = 35°C. Trap temperature = −123 to −125°C. Resonance radiation absorbed = 4.0×10^{-6} einstein per sec. Arc current = 0.100 amp. Arc voltage = 370. Circulation rate = 3 liters per min. Partial ethane pressure = 8 cm. Mercury vapor pressure = 4×10^{-3} mm.*

Run No.	Time, hr.	Initial Pressure, cm	Final Pressure, cm	Percent Hydrogen in Mixture	Fraction of C_2H_6 Reacted	Rate of Disappearance of C_2H_6, Mole per sec. $\times10^6$	Quantum Yield (ethane reacting)	Products, Mols per Mole of Ethane Reacting: H_2 Consumed	CH_4 Formed	C_3H_8 Formed	C_4H_{10} Formed	Higher Hydrocarbons Formed
1	5.5	47.7	47.7	40.0	0.39	0.45	0.11	0.48	1.32	0.07	0.12	none
2	6.0	45.7	45.7	39.3	0.44	0.46	0.12	0.46	1.30	0.08	0.11	none
3	6.0	45.4	45.4	40.0	0.44	0.45	0.11	0.50	1.34	0.05	0.13	none

(c) At very low trapping temperatures where butane has a negligible vapor pressure, and that of propane is also low, hydrogen formation ceases entirely. Propane now makes its appearance in large quantities. This is a striking result, inasmuch as previous investigators have found only hydrocarbons with an even number of carbon atoms (with the exception of methane), and previous mechanisms have been designed primarily for the purpose of explaining this.

(d) It should be observed that, especially at low trapping temperatures where the partial pressure of ethane is low while the methane formed is all in the gas phase, there will be a competition for the incident energy. Under these circumstances the methane present may absorb up to 25 percent of the incident energy. It has been shown by Morikawa, Benedict, and Taylor[7] that the quantum yield in the mercury photosensitized methane decomposition is very low at low temperatures. Thus they obtained values of about 0.2 at 196°C, and only 0.008 at 98°C. It appears, therefore, that the decomposition of methane is negligible at 35°C, and the methane merely quenches the resonance radiation without being chemically affected. On account of this effect the quantum yields obtained will be somewhat low, and a value of about 0.20 for the ethane decomposition at 35°C appears the most probable.

(2) Experiments in the presence of added hydrogen

(a) Hydrogen is consumed, not produced. (b) The production of methane is very large compared with that of higher hydrocarbons. (c) No hydrocarbons higher than butane are formed at low trapping temperatures.

(3) The decomposition of butane

(a) Much hydrogen is produced. The decomposition of butane (and perhaps also that of propane) is thus the source of most of the hydrogen formed in the ethane decomposition at higher trapping temperatures. Higher hydrocarbons are also produced in large quantity. As in the case of ethane, these correspond roughly to octane, but are to some extent unsaturated.

[7] Morikawa, Benedict and Taylor, J. Chem. Phys. **5**, 212 (1937).

(b) The quantum yield of the butane decomposition is definitely higher than that of the ethane decomposition.

Discussion

The following reactions may be considered in discussing the decomposition of ethane and its reaction with hydrogen atoms:

Primary reactions

$$C_2H_6+Hg(2^3P_1)=2CH_3+Hg(1^1S_0), \quad (1)$$

$$C_2H_6+Hg(2^3P_1)=C_2H_5+H+Hg(1^1S_0), \quad (2)$$

$$H_2+Hg(2^3P_1)=2H+Hg(1^1S_0), \quad (3)$$

$$C_2H_6+Hg(2^3P_1)=CH_2+CH_4+Hg(1^1S_0). \quad (4)$$

Secondary reactions of radicals or atoms with ethane

$$CH_3+C_2H_6=CH_4+C_2H_5, \quad (5)$$

$$H+C_2H_6=CH_4+CH_3, \quad (6)$$

$$H+C_2H_6=C_2H_5+H_2, \quad (7)$$

$$C_2H_5+C_2H_6=C_4H_{10}+H, \quad (8)$$

$$CH_3+C_2H_6=C_3H_8+H. \quad (9)$$

Radical and atom recombination reactions

$$2CH_3=C_2H_6, \quad (10)$$

$$CH_3+C_2H_5=C_3H_8, \quad (11)$$

$$CH_3+H=CH_4, \quad (12)$$

$$2H=H_2, \quad (13)$$

$$H+C_2H_5=C_2H_6. \quad (14)$$

$$2C_2H_5=C_4H_{10}. \quad (15)$$

Other secondary reactions of radicals

$$C_2H_5+H_2=C_2H_6+H, \quad (16)$$

$$CH_3+H_2=CH_4+H, \quad (17)$$

$$CH_4+CH_3=C_2H_6+H, \quad (18)$$

$$CH_4+C_2H_5=CH_3+C_2H_6. \quad (19)$$

Reactions involving the methylidene radical

$$CH_2+C_2H_6=C_3H_8, \quad (20)$$

$$CH_2+C_3H_8=C_4H_{10}, \quad (21)$$

$$CH_2+C_2H_6=CH_3+C_2H_5, \quad (22)$$

$$2CH_2=C_2H_4. \quad (23)$$

The ethane decomposition

There are three fundamentally different possibilities for the primary reaction, a C−C bond split (1), a C−H bond split (2), and the elimination of a methylidene radical (4). These will be discussed separately.

(*a*) *The elimination of a methylidene radical.*—This is intrinsically not a very likely mechanism. If (4) were the primary step, it would be possible to account for the products obtained by assuming secondary reactions of the methylidene radical such as (20) and (21). On this basis we would expect the amount of methane to be equal to $(C_3H_8+2C_4H_{10})$, in exact agreement with runs 7 and 8 of Table II. However, since in this case all the butane is formed via propane, we would expect very little butane at the lowest trapping temperatures. This objection might be overcome by assuming (22) followed by (5), (11), and (15). The main objection to (4) as the primary step, however, is the absence of ethylene as a product of the reaction. It seems very unlikely that (4) could be the primary step without any combination of methylidene radicals to form ethylene by (23), especially in view of the low quantum yield of the over-all reaction. The only way to avoid this difficulty would be to assume that at least one of (20), (21), and (22) was extremely fast. On dreierstoss grounds (20) and (21) should not be very rapid. To inhibit recombination to ethylene, therefore, it would be necessary for (22) to have an activation energy much below 7 kcal., which is very unlikely. There would also be the possibility of C_2H_4 formation by the reaction $CH_2+C_2H_6\rightarrow CH_4+C_2H_4$. As a matter of fact Storch and Kassel[8] assume this to be very rapid. It appears, therefore, that (4) is a much less plausible primary step than (1) or (2), and it will not be further considered.

(*b*) *The C−H bond split.*—It is also possible to account for the products of the reaction by assuming an initial C−H bond split (2). If this occurs the most likely fate of the hydrogen atoms produced would obviously be to react with ethane, since it is present in large quantity. We may therefore assume that (6) occurs producing methyl radicals, which react by (5). Recombination reactions (11), (12), and (15) would then yield the experimentally found products. The low quantum yield can be explained partly on the basis of reactions (10) and (14) which regenerate ethane, and perhaps also in part by inefficiency in the primary step (2).

In order that this mechanism shall yield the products found experimentally, it is necessary to assume that reaction (7) is slow compared to (6), since the occurrence of (7) to any appreciable extent would yield far too much butane relative to methane, and would lead to the production of hydrogen, contrary to the experimental findings. Existing estimates of the relative rates of (6) and (7) are conflicting,[9] but it is possible that the necessary conditions are fulfilled.

The above question is, however, of minor importance compared with the main difficulty encountered by any mechanism which assumes a primary C−H split. If such a split occurs, it is necessary to explain the absence of hydrogen from the products, in spite of the possibility of its formation through reaction (13). In other words we must show that (6) can occur rapidly enough to prevent an appreciable fraction of the hydrogen atoms recombining by (13). (For a rough calculation we can neglect the other less important H atom consuming reactions (12) and (14).) We can test this condition by first calculating the average life of a hydrogen atom on the assumption that hydrogen atoms disappear by (6) only, and then ascertaining whether such a life is compatible with the rate of (13).

From the mechanism assumed the number of ethane molecules reacting by (2) to produce hydrogen atoms is approximately $\frac{1}{3}$ of the experimentally found rate of disappearance of ethane. Taking run 7 as an example, we have

C_2H_6 pressure = 7 cm,
quantum yield = 0.15,
energy input = 3.7×10^{-6} einstein per sec.
volume of reaction vessel
= 320 cc.

Hence the rate of production of hydrogen atoms according to this mechanism is

$$(\tfrac{1}{3}\times0.15\times3.7\times10^{-6})/320 = 5.8\times10^{-10} \text{ mole cm}^{-3} \text{ sec.}^{-1},$$

[8] J. Am. Chem. Soc. **59**, 1240 (1937).

[9] Steacie and Phillips, J. Chem. Phys. **4**, 461 (1936); Steacie, ibid., **6**, 37 (1938); Trenner, Morikawa and Taylor, ibid. **5**, 203 (1937).

assuming that the reaction takes place throughout the entire cell. Now if hydrogen atoms disappear by (6) only, the mean life of a hydrogen atom is $1/(k_6(C_2H_6))$. k_6 has been determined by Trenner, Morikawa and Taylor,[9] and by Steacie,[9] who obtained $E=7.2$ kcal., with $s=0.1$, and 8.6 kcal., with $s=0.1$, respectively. Taking the lowest value of E, since it will be the most favorable for removing H atoms from the system, we obtain

$$k_6=3.6\times10^{-8}\text{ cm}^3\text{ mole}^{-1}\text{ sec.}^{-1}\text{ at }35°\text{C.}$$

Hence, since $(C_2H_6)=3.6\times10^{-6}$ mole cm^{-3}, we obtain

$$\text{mean life of a hydrogen atom}=7.7\times10^{-4}\text{ sec.}$$

Now, if recombination occurs, it may be by diffusion of hydrogen atoms to the wall, or by three-body recombination in the gas. Considering only the wall effect, for the moment, we have for hydrogen atoms,

$$D=\tfrac{1}{3}\lambda c,$$

where D is the diffusion coefficient, c the average velocity of a hydrogen atom at 35°C, and λ is the mean free path. Assuming an average pressure in the gas of 7 cm of ethane plus 6.4 cm of methane, we obtain approximately

$$D=9.1\text{ cm}^2\text{ sec.}^{-1}$$

Now the mean displacement ϵ is given by

$$\epsilon^2=2Dt,$$

hence

$$\epsilon=(2\times9.1\times7.7\times10^{-4})^{\frac{1}{2}}=0.12\text{ cm.}$$

Now considering the geometry of the reaction vessel, about 60 cc out of the total volume of 320 cc is within 0.12 cm of the wall, so that on the average one-half of the atoms in this 60 cc will reach the wall during their lifetime. Approximately, therefore, 1/10 of the hydrogen atoms will form H_2 at the wall instead of reacting by (6). The hydrogen formation will therefore be about

$$1/10\cdot\tfrac{1}{2}\cdot5.8\times10^{-10}\text{ mole cm}^{-3}\text{ sec.}^{-1}=2.9\times10^{-11}\text{ mole cm}^{-3}\text{ sec.}^{-1}$$

This is thirty times the minimum detectable amount with the analytical method used. Actually the discrepancy is even greater than this for two reasons. (a) Practically all the incident radiation will be absorbed in the first mm or two of the cell. This will increase the wall recombination by a factor of about 5. (b) Also, we have neglected recombination in the gas, and this will make a considerable contribution. It follows that the amount of hydrogen is probably about 200 times smaller than the C−H bond split mechanism requires.

Processes such as (12) and (14) cannot be invoked to explain the discrepancy, since the slower diffusion coefficients of CH_3 and C_2H_5 will counteract any concentration factors in their favor. Further, the possibility of subsequent consumption of hydrogen by (3), or by the comparatively slow reactions (16) and (17), cannot explain the quantitative absence of hydrogen in the products of the reaction. It must therefore be concluded that if a C−H split occurred as the primary process hydrogen would be a product, and its absence rules out this mechanism.

(*c*) *The C−C bond split.*—It appears, therefore, that the primary process must be a C−C split. In this case the resulting methyl radicals can only react according to (5) yielding ethyl radicals. The various radical recombination reactions will then regenerate ethane (10), or yield butane (15), or propane (11). Such a mechanism gives a complete explanation of the products of the reaction, i.e. large formation of methane and no hydrogen production. The only additional reactions which merit consideration are (18), (9), (8), and (19). (8), (9), and (18) can be eliminated since they produce hydrogen atoms, and in any case the concensus of opinion is that such reactions are slow, thus Morikawa, Benedict and Taylor assign an activation energy of about 16 kcal. to (18). It is also unlikely that (19) should be fast, and in any case its presence would produce little change in the mechanism.

We are thus left with the relatively simple series of reactions (1), (5), (10), (11), and (15). If (10) did not occur, the maximum value of the quantum yield would be 3. The occurrence of (11) will lower the quantum yield, but cannot reduce it below 2. The occurrence of (10), i.e., the recombination of methyl radicals to ethane, will, of course, lower the quantum yield without otherwise affecting the situation. It seems un-

likely, however, that the low yield of 0.2 is to be ascribed entirely to this cause, since diminishing the pressure, and thus increasing the wall-effect, does not lower the quantum yield. It is probable, therefore, that the low quantum yield is to be at least partly ascribed to inefficiency in the primary process (1), perhaps owing to ethane quenching the excited mercury atoms to some extent only to the metastable 2^3P_0 level.

The reaction in the presence of added hydrogen

The quenching cross section of hydrogen for excited mercury atoms is much greater than that of ethane. Thus for hydrogen σ_E^2 is 6.01×10^{-16} cm^2, and for ethane it is 0.42×10^{-16} cm^2, a ratio of about 15 to 1.[10] Furthermore the velocity of hydrogen molecules is about 4 times that of ethane. Hence in 2 : 1 mixtures of hydrogen and ethane, as used in the experiments given in Table IV, hydrogen will absorb about 120 times as much energy as does ethane. Reaction (3) thus becomes the only important primary step.

Since much methane is formed and hydrogen is consumed, we presumably have (6) followed by (5), (10), (11), and (15). Actually, however, about twice as much methane is formed as would be expected on this basis. There are two possible explanations of this. (a) Methyl radicals do not react exclusively by (5), but also disappear by (12) or (17). Of these (12) might occur at the wall sufficiently rapidly to account for the facts. Available estimates of the rate of reaction (17)[11] make it appear to be too slow to be effective. (b) The other possible explanation of the large methane production is that (6) is followed by (5), but that some other reaction of ethyl radicals prevents the exclusive formation of propane and butane. If such a reaction occurs, it must involve hydrogen to explain the difference between the runs in the presence and in the absence of hydrogen. We might thus assume that (16) occurs reforming ethane and regenerating a hydrogen atom. On such a basis we can account for the products formed. Of course this involves the assumption that (16) occurs rapidly enough. What evidence there is seems to be against this, and indicates an activation energy of about 15 kcal.[12] It is worth noting that if (16) is postulated in this way there is no need to rule out (7) as an alternative reaction step to (6), since if (7) were largely followed by (16) the net stoichiometric result would be zero. The same result might also be arrived at by assuming reformation of ethane by (14).

It is hoped that further work now in progress on the reaction at high temperatures, and in the presence of deuterium, may enable a decision to be made between some of the various alternative mechanisms discussed above.

The reaction at high trapping temperatures

Under these circumstances the reaction is complicated by secondary processes, and the results are thus only of minor importance. Since the addition of hydrogen to ethane at low trapping temperatures leads to hydrogen consumption rather than production, it is apparent that the production of hydrogen from ethane alone at high trapping temperatures is not "auto-catalytic," and must be due to secondary decomposition of butane. Also, the low methane production relative to the butane and higher products formed must be due to the presence of butane. It thus appears that the butane decomposition leads to the formation of higher products from ethane in some manner not involving the production of methane.

The decomposition of butane

Since these experiments were made merely to confirm the production of hydrogen, no discussion is necessary. In any case an investigation of the butane decomposition in the near future is contemplated. The propane decomposition is at present under investigation.

[10] Bates, J. Am. Chem. Soc. **52**, 3825 (1930).

[11] Trenner, Morikawa and Taylor, J. Chem. Phys. **5**, 203 (1937); v. Hartel and Polanyi, Zeits. f. physik. Chemie **B11**, 97 (1930); Sickman and O. K. Rice, J. Chem. Phys. **4**, 608 (1936); Patat, Zeits. f. physik. Chemie **B32**, 274 (1936); Paneth Hofeditz and Wunsch, J. Chem. Soc. 372 (1935).

[12] Leermakers, J. Am. Chem. Soc. **55**, 4508 (1933).

Effect of Electric Fields on the Decomposition of Ammonia by Alpha-Rays

CATHERINE SMITH AND HARRY ESSEX
Department of Chemistry, Syracuse University, Syracuse, New York
(Received January 27, 1938)

The following values have been obtained for the ion yields in the alpha-ray decomposition of gaseous ammonia in the absence and presence of electric fields at 30°C and 100°C:

30°C	no field	1.37
	half-saturation	1.17
	full saturation	1.08
100°C	no field	2.42
	half-saturation	2.06
	full saturation	2.01

The results are interpreted upon the hypothesis that in a field sufficiently strong to produce half-saturation, the ions are neutralized upon the plates without decomposition. If this hypothesis is correct, of the ion yield 1.37 at 30°C, 0.40 is the ion yield due to recombination of ions and 0.97 the ion yield due to other mechanisms. Similarly of the ion yield 2.42 at 100°C, 0.72 is the ion yield due to recombination of ions and 1.70 the ion yield due to other mechanisms. Possible mechanisms of that part of the reaction consequent on ion recombination and of that part of the reaction independent of ion recombination are discussed.

IN the passage of alpha-particles through a gas both primary and secondary ionization result. The primary ionization is due to collisions of alpha-particles with molecules and the liberated electrons may have velocities between 0 and $2V$, where V is the velocity of the alpha-particle. If the speed of the ejected electrons is sufficiently high, they may in turn produce a number of ions before they come to rest. The number of ions produced by secondary ionization is approximately four-fifths of the total ionization.[1, 2] However, the total energy of the alpha-rays is frequently more than twice the energy used in ionization and it is known that some of this energy produces excited or metastable molecules. The collision of an alpha-particle with a molecule may also directly split the molecule into radicals or atoms.

Some photochemical reactions are known to be initiated by excited molecules which decompose either directly or on collision with a neutral molecule. This type of mechanism is represented by the photochemical decomposition of ammonia.[3] Other reactions produced by light occur due to the immediate splitting of the irradiated molecule, as with chlorine in the synthesis of hydrogen chloride from the elements.[4]

These mechanisms which have been used to explain photochemical reactions also seem plausible in alpha-ray decomposition. Or metastable molecules may decompose on collision with other molecules. Sufficient energy is liberated on the neutralization of ions to initiate chemical reaction. Reaction may occur on the neutralization of ions (clustered or not) or on ions before neutralization. One or the other of these mechanisms, or a combination of two or more, has been used by different investigators to explain reactions initiated by alpha-rays.

If some of the ions could be removed from the gas before neutralization, the value of the ion yield determined under such conditions might give some indication as to the mechanism of the reaction. Essex and FitzGerald[5] successfully determined the ion yield in the decomposition of ammonia by alpha-rays using the saturation current method to determine the number of ions produced. Their work suggested the possibility of determining the yield in electric fields sufficient to produce saturation, that is, under conditions under which recombination of ions in the gaseous phase does not occur. This paper is a report of ion yield measurements in the decomposition of ammonia by alpha-rays in the presence and absence of strong electric fields. The ion yields are compared and possible mechanisms discussed.

[1] Rutherford, Chadwick and Ellis, *Radiations from Radioactive Substances*, p. 145.
[2] H. Bethe, Ann. d. Physik **5**, 400 (1930).
[3] E. O. Wiig and G. B. Kistiakowsky, J. Am. Chem. Soc. **54**, 1806 (1932).
[4] M. Bodenstein and Taylor, Zeits. f. Elektrochem. **22**, 53 (1916).
[5] H. Essex and D. FitzGerald, J. Am. Chem. Soc. 56, 65 (1934).

Experimental Details

The apparatus is represented diagrammatically in Fig. 1. It was constructed of Pyrex glass, except for the reaction vessel through which the heavy platinum leads to the platinum electrodes were sealed. The electrodes were 4 cm in diameter. The cylindrical vessel, 11 cm long and 6.5 cm in diameter, was blown of soft glass and was connected to the rest of the system by a graded seal. To prevent electrical discharge between the electrodes and the glass walls and also to prevent current conducted through and over the glass from inclusion in the ion current, thin copper disks were cemented to both ends of the reaction vessel. The cement used was a mixture of "Liquasol" and finely powdered silver. The disk at the high potential end was 5 cm in diameter and electrically connected to the high potential lead. The disk at the low potential end, 3 cm in diameter was provided with a hole 5 mm in diameter through which passed the lead to the low potential electrode. This disk was grounded. The radioactive material, an isotopic mixture of radium and mesothorium was placed in the depression of the reaction vessel and the vessel was surrounded by an air bath maintained at constant temperature.

The ammonia was obtained from a solution of ammonia in ammonium thiocyanate and was dried as it passed over crushed potassium hydroxide and barium oxide. Previous to introducing an ammonia sample, the entire system was evacuated by means of a mercury vapor pump to a pressure of less than 10^{-5} mm as measured by the McLeod gauge. While the system was being evacuated, trap T' was surrounded with liquid air[6] and dry ammonia was admitted. When sufficient ammonia was condensed to fill the apparatus at more than the desired pressure, the stopcock to the generator was closed and evacuation continued until the pressure with the pump in operation, was again less than 10^{-5} mm. The liquid air was then removed and the ammonia allowed to evaporate, the first portion to vaporize being withdrawn through the pump. Then the stopcock to the pump was closed and the remaining ammonia allowed to vaporize. After vaporization was complete the ammonia was again condensed, the stopcock to the pump was opened when the condensation was nearly complete and the last fraction not yet condensed was removed through the pump. This procedure of successive vaporization, condensation and evacuation was repeated three or four times until the pressure at equilibrium after freezing out the ammonia was less than 5×10^{-5} mm. The liquid air was then placed around trap T, enough ammonia condensed there to fill the apparatus at more than the desired pressure and the connection to the ammonia reservoir sealed at d'. This sample was then vaporized and enough ammonia withdrawn to give the desired pressure (calculated from the volumes of the system before and after sealing). The remaining ammonia was again condensed and the system evacuated to a pressure of 10^{-6} mm and the pump sealed off at d.

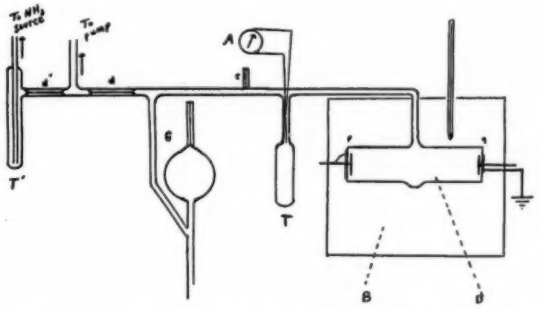

FIG. 1. T' and T, Traps for condensing out ammonia; d' and d, Pyrex barometer tubing; G, McLeod gauge, volume of bulb = 108.7 cc, radius of capillary = 0.443 mm; A, thermocouple and millivoltmeter; c, capillary, used to open system; B, constant temperature air bath; D, reaction vessel, length = 11.0 cm, diam. = 6.5 cm, vol. = 339 cc, electrode distance = 10.2 cm; p, high potential end of vessel; q, grounded end of vessel.

The electrical connections are shown in Fig. 2.

With the system filled at the desired pressure, the transformer was run up to 20,000 volts, the switch tripped and readings taken on the galvanometer and the electrostatic voltmeter as the potential dropped. Characteristic curves obtained on plotting galvanometer deflections versus voltage are shown in Fig. 3. That the great majority of the positive ions arrived at the plate is indicated first by the fact that the current reached a constant value at high potentials. Second, separate experiments were carried out

[6] The liquid air used in this investigation was provided by the General Electric Company of Schenectady, New York, through the courtesy of Dr. L. M. Willey, to whom the authors wish to express their gratitude.

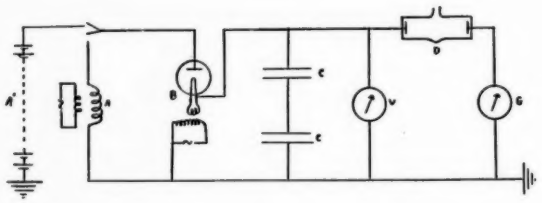

FIG. 2. A', storage battery, 1071–1118 volts; A, transformer, G.E. type K, form E, capacity 3kva; B, rectifying tube, G.E. Kenetron, type KP-2, voltage on primary of filament transformer (11 to 1 ratio) 70; C, condensers, G.E., capacity = 0.25 mf, 18,000 volts; V, electrostatic voltmeter, G.E. type EL-2, 30,000 volts; D, glass vessel, platinum electrodes; G, galvanometer, L+N type R, internal resistance = 516 ohms, sensitivity = 1×10^{-10} amp./mm at 1 meter.

for evidence of arrival of ions at the glass. With the galvanometer inserted between the low potential shield and the ground, the current to this shield both in the absence and presence of radioactive material was measured. No difference was observed. Third, the ion yields obtained in the absence of fields agree with those obtained by other investigators.

After thirteen or more hours the ammonia was frozen out and the residual pressure measured after ten minutes. The liquid air was kept around the trap for about an hour during which time the residual pressure was frequently measured. In none of the runs was any change in pressure observed during this time. The time at which the ammonia was again vaporized was considered as the starting time of the reaction, pressure changes thereafter being assumed to be due only to ammonia decomposition. The nitrogen and hydrogen were considered to be present in stoichiometric proportions.[7–9] Current-potential curves were taken at regular intervals during the run. Subsequent to each set of current measurements the galvanometer was calibrated. This was accomplished by determining with a potentiometer the potential necessary to give the same swings through a known resistance. In the runs at 100°C the pressure was such that the gas density was the same as in the runs at 30°C.

In calculating the rate of decomposition from the pressure changes, the different temperatures of the various portions of the system were taken into account. Pressure correction for these effects was determined in the following manner. A drying tube filled with soda-lime was sealed on to the capillary c through a stopcock. After the system had been thoroughly evacuated and sealed at d, dry air was admitted to a low pressure, where the simple gas laws hold with considerable accuracy, and the stopcock was closed. The pressure of the air in the system was read on

[7] E. Wourtzel, Le Radium **11**, 332 (1919).
[8] A. Koenig and Th. Brings, Zeits. f. physik. Chemie, Bodenstein Festband, 541 (1931).
[9] A. Luyckx, Bull. soc. chim. Belg. **43**, 160 (1934).

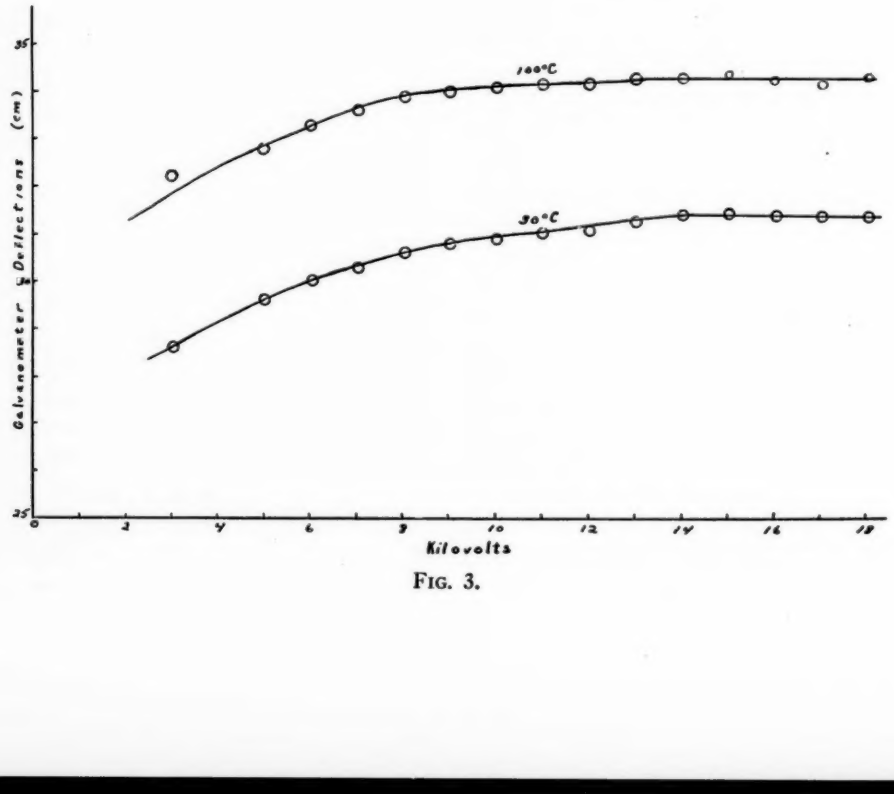

FIG. 3.

the manometer formed by the tube leading to the McLeod gauge and by the leveling bulb. Then liquid air was placed around trap T and its level adjusted to contact with the attached thermocouple. After ten minutes the pressure of the air was again read. It follows from the gas laws that the relation between P, the pressure without the liquid air around the trap and P_L, that with the liquid air is

$$P=P_L\frac{V_tT_r+V_sT_L-V_tT_L}{V_sT_L},$$

where V_t is the volume of the trap at liquid-air temperature, V_s is the total volume of the system, T_r is room temperature and T_L is the temperature of the trap partly immersed in liquid air. V_s, V_t, T_r and T_L are constants. Hence the above relation reduces to

$$P=KP_L.$$

The value of K determined in the above manner was found to be 1.23 when the bath was at 100°C and 1.16 when it was at 30°C. Because of the low pressure (approximately 10 cm) these values determined for air hold accurately for nitrogen-hydrogen mixtures. This correction was applied to all the residual pressure readings with ammonia. At this pressure P, 349 cc of the nitrogen-hydrogen mixture were at the temperature of the bath and 222 cc at room temperature.

The greatest known uncertainty in the experimental measurements from which the ion yields were calculated was in the pressure measurements. Assuming an uncertainty in reading the McLeod gauge of 0.5 mm, the probable error in yields does not exceed 3 percent.

The experimental data and the calculated ion yields are presented in Table I. A sample calculation follows. The results are shown graphically in Fig. 4.

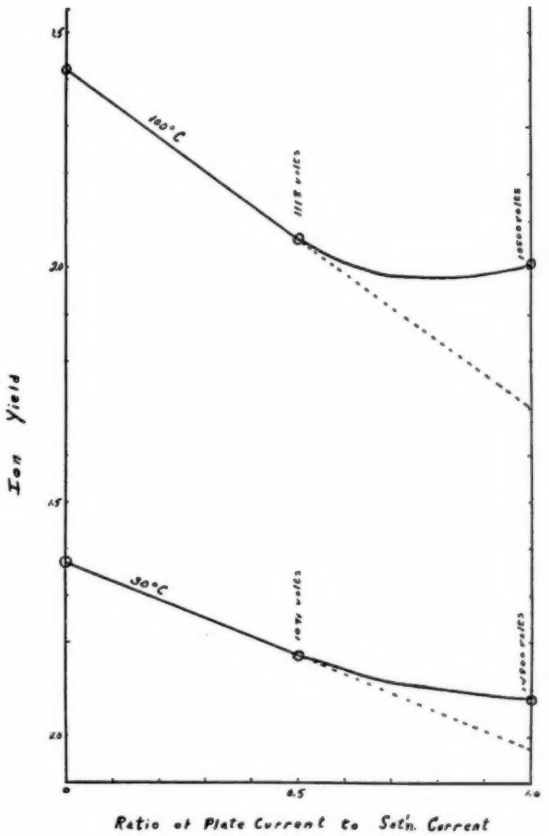

FIG. 4. Since the potential for half-saturation is but 0.1 of that for saturation, the curve to half-saturation is drawn as a straight line.

Sample calculation (For run at 100°C and no field)

M—Number of gram mole of ammonia decomposed.

Number g mole of N_2+H_2 in 348 cc

$$=\frac{0.0435\times348}{760\times82.1\times373}=6.50\times10^{-7},$$

TABLE I.

Temp. °C	Press. of NH_3 (cm)	Potential (volts)	*Duration (hours)	Residual Pressure Change (mm)	Room Temp.	Current amp. $\times10^{-8}$		Ion Yield
						Satn.	To Plate	
30	62	0	173.7	0.0345	23°C	5.92	0	1.37
30	62	1071	118.5	0.0196	22	5.79	2.88	1.17
30	62	14900	124.2	0.0201	23	6.10	6.10	1.08
100	76	0	125.0	0.0435	22	5.21	0	2.42
100	77	1118	126.1	0.0352	24	4.89	2.49	2.06
100	76	10500	70.1	0.0186	27	4.71	4.76	2.01

* The duration of the run was obtained by substracting from the total time the time during which the ammonia was condensed.

Number g mole of N_2+H_2 in 222 cc

$$=\frac{0.0435\times 222}{760\times 82.1\times 295}=5.25\times 10^{-7},$$

$$M=\frac{(6.50+5.25)\times 10^{-7}}{2}=5.88\times 10^{-7}.$$

N—Number of gram ions present.

$$\text{Number amp.}=5.21\times 10^{-8},$$

$$\text{Number coulombs}=5.21\times 10^{-8}\times 125.0\times 3600,$$

$$N=\frac{5.21\times 10^{-8}\times 125.0\times 3600}{96500}$$

$$=2.43\times 10^{-7}.$$

$$M/N\text{—Ion yield}=\frac{5.88\times 10^{-7}}{2.43\times 10^{-7}}=2.42.$$

Preliminary experiments were carried out in which the residual pressure was measured as a function of time in the absence of radioactive material both in the absence and presence of electric fields. The observed residual pressure changes were small and equal to zero within the experimental error of these measurements. It may be assumed, therefore, that decomposition due to catalysis and electric discharge plays a negligible part in the measured reaction.

Ion yields were initially determined by the described procedure using a vessel in which about one-third of the volume was behind the plates and without exterior shields. The results shown in Table II were obtained.

In these preliminary experiments the ion yield in no field at 100°C was very much higher than that obtained by others and it was found that the saturation current at 100°C was only about 68 percent of that at room temperature, even when precautions were taken not to unnecessarily disturb the distribution of the radioactive material. Temperature[10] should affect but slightly the number of ions produced by the alpha-particles at constant density. However, temperature does affect the velocity of diffusion of the emanation and it seems likely that at 100°C a large fraction of the ions from the emanation and its decomposition products were being produced behind the plates where the field strength was low and insufficient to bring all of them to the plates, before recombination. Hence the calculated value of the number of ions formed by the radioactive material was low. The conductivity from plate to plate in the absence of ionizing radiations was negligible with this vessel. Apparently the specific resistance of the glass used was a great deal higher than that from which the final reaction vessel was constructed.

To avoid errors from the indicated source the reaction vessel used in the final measurements was constructed with the electrodes as close to the ends as practical without contact. Preliminary experiments with such a vessel, however, showed the presence of slight discharges between the electrodes and the glass. Errors of this sort were eliminated by the copper shields.

Even with the final vessel the saturation current at the higher temperature was only about 90 percent of that at 30°C. The space behind the electrodes was too small to account for this discrepancy. It is believed that the major portion of this difference is due to removal by convection currents of a larger quantity of the emanation and, therefore, of its decomposition products from the reaction vessel to the connecting tube at the higher temperature. The connecting tube projected vertically upward from the reaction vessel through the cover of the constant temperature air bath. Considerable convection might result from the large temperature gradient within a few centimeters of the reaction vessel. Some error may result but it should not be large as the paths of the alpha-particles produced in the connecting tube are greatly shortened and hence the number of ions not brought to the plates is small.

TABLE II.

	Room Temp.		100°C	
	Voltage	Ion Yield	Voltage	Ion Yield
No field	0	1.25	0	3.10
50% sat'n.	765	1.16	383	2.65
98% "	—	—	4600	2.51
100% "	17000	1.09	10300	2.76

[10] A. Becker and Ilsemarie Schaper, Zeits. f. Physik **79**, 186 (1932); **91**, 422 (1934).

Discussion of Results

Ion yields in absence of electric fields

The ion yields here reported of 1.37 at 30°C and 2.42 at 100°C give a temperature coefficient of 0.015 units per degree. They were obtained at extremely low intensities of ionization. Ion yields to be found in the literature, with the exception of the earlier and more qualitative values obtained by Essex and FitzGerald[5] in this laboratory, are at much higher intensities of irradiation, in most cases several hundred times as great, and cannot, therefore, be directly compared.

Luyckx[11] has, however, in a recent careful and accurate work determined the effect of intensity of ionization in the ammonia decomposition at 19°C and has extrapolated his data to zero intensity. As the lowest intensity at which he measured the ion yield in the neighborhood of atmospheric pressure is approximately thirteen times as great as in these experiments, the Luyckx value to be used for comparison is the extrapolated value at zero intensity. It is 1.27 at 19°C or 1.27 $(1+0.015\times 11)$ at 30°C which equals 1.44. This value compares favorably with 1.37 obtained in the present study. Luyckx made no measurements at higher temperatures. If, however, the effect of intensity can be assumed the same at 100°C as at 19°C, the limiting value of the ion yield may be approximated at 100°C by the following relation

$$0.87 : 1.27 = 1.63 : (M/N_\infty)_{100°C},$$

where 0.87 and 1.63 are the interpolated values at 19°C and 100°C, respectively, based on the values Jungers[12] obtained on the recalculation of Wourtzel's[7] results. The ion yield at 100°C and at limiting intensity is thus found to be 2.38 as compared with the present value of 2.42. The effect of intensity at temperatures other than room temperature has not been studied. Jungers[13] in a study of the effect of temperature on the ion yields for the decomposition of ammonia and deutero-ammonia, reports that the yield for ammonia at 100°C and 52.5 mm is 1.87 times that at 20°C.

[11] A. Luyckx, Bull. soc. chim. Belg. **43**, 117 (1934).
[12] J. C. Jungers, Bull. soc. chim. Belg. **41**, 377 (1932).
[13] J. C. Jungers, J. Phys. Chem. **40**, 155 (1936).

The direct method of ion yield determination used in this laboratory eliminates many uncertainties which enter into other methods involving, in the method of homogeneous irradiation, the assumption of the validity of Geiger's law, and depending on the accuracy of the hypotheses used regarding the distribution of the Ra A and Ra C′ between the walls and the gas, on the values assigned to the ranges and resulting ionization of the various alpha-particles and on calculations regarding the effect of recoil atoms. Where the effect has been taken into account at all, the methods of correcting for the unequal distribution of the ionization along the trajectory of an alpha-particle appear particularly doubtful. Most of these sources of error are also present in the method of central irradiation, together with the errors involved in the determination of the decrease in range of an alpha-particle due to the thickness of the central glass bulb containing the radon.

The effect of electric fields

The data, here presented, are the first regarding the effect of electric fields on the ion yield. In a field less recombination of ions occurs in the gaseous phase and in a saturation field no recombination of ions can take place in the gas. The results show that as the field is increased, the first effect is to decrease the ion yield. The decrease in the yield, however, is not proportional to the current (Fig. 4), an effect particularly marked at the higher temperature, indicating at high potentials the initiation of a new mechanism of decomposition or the increase in efficiency for decomposition of a reaction already taking place.

Due to the presence of other molecules and atoms to take up the energy, the neutralization of ions at a plate might be expected to result in less decomposition than in the gaseous phase. If it is assumed that the low fields result in neutralization at the plate without decomposition, the ion yield due to recombination of ions in the gas phase can be calculated from the results. Considering the values at 30°C, at which the ion yield in no field is 1.37 and that at half-saturation is 1.17 (a difference of 0.20), the ion yield due to the recombination of ions is 0.40. An analogous calculation at 100°C leads to an ion yield due to

recombination of ions of 0.72. Decomposition per ion pair due to other mechanisms than ion recombination is calculated on this assumption to be at 30°C, $1.37-0.40=0.97$ and at 100°C, $2.42-0.72=1.70$. It is to be noted that the voltage for half-saturation is only about one-tenth that for full saturation.

Mechanism

Decomposition of ammonia in the presence of alpha-rays would certainly be expected to take place by other mechanisms than ion recombination. As only a relatively small fraction of the energy of alpha-rays is used in ion production, a considerable portion of this energy must go into producing excited molecules. Studies of the photochemical decomposition and of the absorption spectrum of ammonia show fairly definitely that excited molecules of ammonia decompose spontaneously to NH_2 and H. All recent work on the photochemical decomposition of ammonia postulates this as the first step.[3, 14–16]

Duncan[17, 18] in studying the absorption spectrum of ammonia, has shown the presence of four band systems, the first of which is due to the displacement of electrons to the first excitation level. This system shows no line structure in the bands and is of the type known as "predissociation," which have been interpreted as indicating that spontaneous dissociation immediately follows excitation to this stage. The other three band systems show line structure, which indicates that spontaneous dissociation does not occur from higher excited states. Dissociation might, however, occur on collision of ammonia molecules in these higher excited states with neutral molecules. In the far ultraviolet the absorption spectrum is continuous which indicates that ammonia molecules are decomposed directly by high energy quanta probably, according to Duncan, into N and 3H. Molecules of ammonia excited to the first level should then decompose spontaneously, those excited to higher levels might decompose on collisions or spontaneously after the fall of the displaced electron to the first level. If this occurs, fluorescence should be observed. Duncan is studying the visible and near ultraviolet region for evidence of fluorescence. Electrons of energies equivalent to the quanta which are responsible for continuous absorption might be expected to produce direct dissociation in the manner indicated.

Still other mechanisms of ammonia decomposition are possible. Mund,[19] for instance, considers that decomposition may occur in the molecules clustered about an ion before neutralization. Such a mechanism seems to explain most satisfactorily the synthesis of hydrogen chloride from hydrogen and either positive or negative chlorine ions produced by a point discharge.[20] In this case Gunther and Holm believe that a chlorine ion attaches chlorine molecules to itself and that the chlorine molecules dissociate on the surface of the cluster. The atoms thus formed start chain reactions with the hydrogen. However, a mechanism of this kind appears less probable for reactions requiring considerable energy of activation.

According to modern theory, by far the larger part of the energy lost by the passage of charged particles through gases is lost in inelastic collisions. In the case of alpha-ray ionization for air approximately four-fifths[1, 2] of the ionization is secondary, that is, due to inelastic collisions of electrons with molecules. Lunt and Meek[21] have calculated, for the passage of electrons through hydrogen, the distribution of the energy loss among ionization, excitation, vibration and elastic collisions. If the distribution of the energy loss of electrons in collisions is assumed the same in passing through ammonia as is passing through hydrogen, approximately 8 percent of the energy of an alpha-particle is used up primarily in elastic collisions and 92 percent is distributed among ionization, excitation and direct decomposition. Since 11.3 ev[17] is the ionization potential

[14] H. W. Melville, Trans. Faraday Soc. **28**, 885 (1932).
[15] R. A. Ogg, P. A. Leighton and F. W. Bergstrom, J. Am. Chem. Soc. **56**, 318 (1934).
[16] L. Farkas and P. Harteck, Zeits. f. physik. Chemie **B25**, 257 (1934).
[17] A. B. F. Duncan, Phys. Rev. **47**, 822 (1935).
[18] A. B. F. Duncan and G. R. Harrison, Phys. Rev. **49**, 211 (1936).
[19] W. Mund, *L'Action Chimique des Alpha Rayons en Phase Cazeuse* (Hermann et Cie, Paris, 1935).
[20] P. Gunther and K. Holm, Zeits. f. physik. Chemie **B33**, 407 (1936).
[21] R. W. Lunt and C. A. Meek, Proc. Roy. Soc. A157, 146 (1936).

of ammonia and approximately 37 ev[22] is expended in the formation of an ion pair in ammonia, 11.3/37 or 31 percent of the energy goes into ionization. Hence the remaining 61 percent or 0.61×37 which equals 23 ev goes into excitation. Assuming that the balance of the energy goes entirely into excitation at the first excitation level, 23/6.2[23] or 3.7 excited molecules are produced per ion, which on the basis of our data at 30°C would mean an excited molecule yield of 0.97/3.7 or 0.26. This is considerably greater than the quantum yield of 0.18[24] obtained in the photochemical decomposition of ammonia at ordinary temperatures and atmospheric pressure. This discrepancy can be accounted for upon the assumption that the energy of the alpha-particle which goes neither directly into ionization nor into kinetic energy is distributed between excitation and direct decomposition. The latter energy should be of high efficiency, if the decomposition is that postulated by Duncan, namely to N and 3H. It is of interest to note that a quantum yield of 0.69 was found by Kassel and Noyes[25] in the photochemical decomposition of ammonia at wave-lengths of 1600 to 1900A. Gedye and Rideal[26] suggest that this higher yield may be accounted for by the decomposition of the more highly excited molecules to NH and 2H, a reaction for which the quantum energy is sufficient at these wave-lengths. On the basis of Duncan's recent work this seems improbable, but the greater efficiency may be accounted for by collisions between molecules in the higher excited state and neutral molecules. However, in a recent paper Groth[27] working in the Schumann region of the ultraviolet reports an ion yield in the ammonia decomposition of 0.17 at 1470A and 1295A in complete agreement with the result of Wiig[24] at 2000A. This appears more probable. 1295A is still above the region of continuous spectrum and the corresponding quantum energy is insufficient for the decomposition to N and 3H.

If the spectrum of ammonia and its photochemical decomposition have been correctly interpreted, it would appear probable that the mechanism of the reaction involved in the recombination of ions should be similar to that proposed for excited molecules. The recombination may take place, at least to some extent, in the falling of an electron to the first excited level followed by spontaneous decomposition or the electron may fall in directly with resulting decomposition to N and 3H, for which apparently, as the absorption spectrum becomes continuous at frequencies below that corresponding to the ionization potential, sufficient energy is available. A combination of these two methods of neutralization would be expected to result in an ion yield above the quantum yield of 0.18. The value calculated from the results of this work and on the basis of the stated assumptions is 0.40. If, before neutralization occurs, the positive ion has surrounded itself with neutral molecules to form a cluster, or if, as should happen after a longer interval due to the small electron affinity of ammonia, the neutralization is that of a positive cluster by a negative ammonia ion, the mechanism of the resulting reaction might be different, or the same. There seems to be no evidence available bearing on this point.

Bartlett[28] has carried out experiments in which electrons were accelerated into ammonia at low pressures and the resulting ions after acceleration by an electric field were analyzed by a magnetic field using the Dempster method. No negative ions were found. The positive ions produced were NH_3^+, NH_2^+ and NH^+. The variation in the intensity of the NH^+ and NH_3^+ lines with pressure showed definitely that the NH^+ ions were the result of collisions of NH_3^+ ions with neutral molecules. The NH_3^+ and NH_2^+ ions were both primary products produced by electrons of about the same energy, 11.2 and 12.0 ev, respectively, and in about equal numbers.

This work of Bartlett's indicates that in the passage of alpha-rays through ammonia, particularly as most of the ionization is by electrons, the primary ions are NH_3^+ and NH_2^+ in about equal numbers.

Taylor[29] in a study, by means of a modified

[22] Rutherford, Chadwick and Ellis, *Radiations from Radioactive Substances*, pp. 81 and 82.
[23] R. S. Mulliken, J. Chem. Phys. **1**, 492 (1933).
[24] E. O. Wiig, J. Am. Chem. Soc. **57**, 1559 (1935).
[25] L. S. Kassel and W. A. Noyes, J. Am. Chem. Soc. **49**, 2495 (1927).
[26] G. R. Gedye and E. K. Rideal, J. Chem. Soc. 1160 (1932).
[27] W. Groth, Zeits. f. physik. Chemie **37**, 307 (1937).
[28] J. H. Bartlett, Phys. Rev. **33**, 169 (1928).
[29] D. D. Taylor, Phys. Rev. **47**, 666 (1935).

Aston type mass spectrometer, of the ions produced in ammonia by controlled electron collisions also found no NH^+ at low electron energies and low pressures. Since in fields of the strength used in the present work, the kinetic energies of the ions are not appreciably greater than the thermal energies of the surrounding molecules,[30] it is doubtful that NH^+ ions are produced by collisions.

If the simple interpretation which has been given to the results in electric fields is to hold, the ions neutralized on the plates must regenerate ammonia. Neutralization of the positive ions NH_3^+ and NH_2^+ in the presence of other atoms or molecules to remove the excess energy may result in the following reactions with the direct or indirect regeneration of ammonia.

$$NH_3^+ + \theta + M \rightarrow NH_3 + M \quad (1)$$

$$NH_2^+ + \theta + M \rightarrow NH_2 + M \quad (1a)$$

$$NH_2 + H + M \rightarrow NH_3 + M \quad (2)$$

$$NH_2 + NH_2 + M \rightarrow N_2H_4 + M \quad (2a)$$

$$N_2H_4 + H \rightarrow NH_3 + NH_2 \quad (2a')$$

These reactions are plausible on the basis of photochemical results. The quantum yield falls off very rapidly at low pressures. Wiig[31] proposes the occurrence of reactions (2) and (2a) followed by (2a′) to account for the decrease in quantum yield at pressures of ammonia below 100 mm, assuming that at these low pressures the reaction becomes heterogeneous and regeneration of ammonia occurs on the walls.

When the negative ammonia ions are neutralized, energy is required to remove the electron from the molecule and no chemical action can occur.

The reaction apparently initiated or greatly accelerated by high voltage must be due either to increased efficiency for decomposition of collisions of the ions on the plates or of collisions of the ions with gaseous ammonia molecules. The present work yields no information favoring either one or the other of these mechanisms. By increasing the life of the ions at the same potential gradient, information might be obtained bearing on this question. This might be accomplished by using a reaction vessel of the same general design but with a greater distance between the electrodes. The ions being removed to the plates would undergo more collisions due to the greater distance traveled. If the change in yield is due to increased efficiency of collisions of the ions with the plate, the yield in a vessel of this design should be the same as in the present work but if it is due to increased efficiency of collisions of ions with molecules, it should be greater.

An increase in temperature in both the photochemical[15, 32] and radiochemical decomposition of ammonia results in a large increase in yield. In the present work the true ion yield is found to increase from 0.40 at 30°C to 0.72 at 100°C, and the ion yield due to other mechanisms, assumed to be mostly initiated by excited molecules, from 0.97 at 30°C to 1.70 at 100°C. In both cases the yield at 100°C is 1.8 times that at 30°C which is in conformity with the hypothesis that the primary and, therefore, also secondary mechanisms resulting from ion recombination and excited molecules are similar.

The results of this work show that by the study of radiochemical reactions in electric fields, the part of the reaction due to recombination of ions may be separated, at least to some extent, from that part due to other mechanisms. With some reactions the separation may be complete.

[30] See for instance, Darrow, *Electrical Phenomena in Gases* (1932), p. 195.
[31] E. O. Wiig, J. Am. Chem. Soc. **59**, 627 (1937).
[32] W. Kuhn, Comptes rendus **177**, 956 (1923); **178**, 708 (1924).

Infra-Red and Raman Spectra of Polyatomic Molecules

I. An Automatic Prism Spectrometer for the Infra-Red

HAROLD GERSHINOWITZ AND E. BRIGHT WILSON, JR.
Mallinckrodt Chemical Laboratory, Harvard University, Cambridge, Massachusetts

(Received January 31, 1938)

A spectrometer has been constructed which contains two prisms, one of NaCl, the other of KBr, each in a Wadsworth-Littrow mounting. The prisms may be interchanged in the optical train without opening the spectrometer housing or disturbing the calibration. The recording system includes a Barnes-Matossi type amplifier using a photronic cell. The recording is done stepwise, so that the zero of the amplifying system, the intensity of the source and the intensity of transmitted radiation are measured at each setting of the prism table, which is moved by a ratchet device.

THE design of the spectrometer to be described was largely determined by the purpose it was meant to fulfill. The spectrometer is one of a number of different types of apparatus whose combined function is to determine the thermodynamic properties of organic molecules. An instrument was desired that would be capable of determining the fundamental vibration frequencies of these molecules, require as little attention as possible and at the same time be sufficiently flexible to permit the use of absorption cells of many different sizes and the heating of these cells if necessary.

Since practically all of the molecules in which we are interested have fundamental vibrations of lower frequencies than can be reached with a rocksalt prism, it was necessary to use a prism of potassium bromide in addition. A considerable advantage in economy of construction and operation has been achieved by incorporating both prisms into the same mounting and housing by means of a rotating top on the prism table. This and the noncontinuous type of recording which has been employed are the principal new features of the instrument.

The spectrometer is designed after the combination Wadsworth-Littrow type, in which the radiation passes through the prism twice at approximately minimum deviation. Fig. 1 shows schematically the optical arrangement. L_1 is

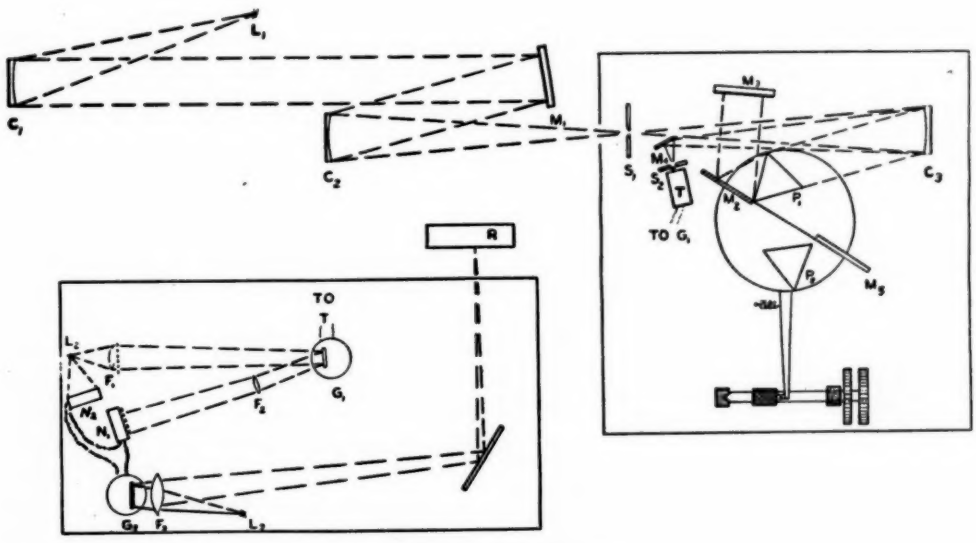

FIG. 1. Diagram of apparatus.

the light source, which is a Globar.[1] It was found that a completely satisfactory mounting for the Globar could be constructed by using the full 6″ length with the standard commercial spring clip terminals. A brass frame was built to hold the spring terminals and the assembly was inserted into an iron pipe 4″ in diameter, which was wound with copper tubing through which water is circulated. Good contact between the pipe and tubing was secured by means of a cement of water glass and magnesia. A slit in the pipe permits radiation to emerge. C_1 is a concave mirror which gives a beam of parallel light into which the absorption cells are inserted. L_1 and C_1 are fixed with respect to each other and mounted on a base that may be moved with respect to M_1, so that different size cells may be inserted. M_1 is a plane mirror and C_2 a concave mirror which focuses the light on the entrance slit S_1.

The following parts, which constitute the spectrometer proper, are all enclosed in a well-insulated box[2] represented by the solid frame in Fig. 1: the entrance slit S_1, the collimating mirror C_3, the two prisms P_1 and P_2 the two Wadsworth mirrors M_2 and M_5, the Littrow mirror M_3, the small plane mirror M_4, the exit slit S_2 and the thermopile T. The slits may be operated from outside the thermostat by rods that run through tightly fitting rubber tubing. The thermopile, which is attached to the exit slit S_2, is enclosed in an evacuated glass jacket and surrounded by an iron pipe and is lagged with felt. The leads from the thermopile to the galvanometer G_1 are single lengths of copper wire, twisted and run through a copper tube. G_1 is surrounded by shields of copper and soft iron and is lagged with cotton waste and felt. The prism table can be set in either of two positions 180° apart from outside the thermostat by means of strings. The prism table is turned by means of an arm 10″ long which is held by a spring against a flat on a long nut which moves on a 1″ diameter, 1 mm pitch screw. The nut has a tail which runs in a groove and keeps it from rotating. The screw is turned by a ratchet and pawl driven from outside the spectrometer by a string. All the strings that run into the spectrometer pass through $\frac{1}{8}$″ copper tubing packed with heavy grease, which seals the inner box from the atmosphere. One notch on the ratchet moves the prism table 10″ of arc. The screw is geared to a Veeder counter outside the thermostat. One notch on the ratchet corresponds to one Veeder number. The prism table may be moved continuously instead of stepwise by the shaft that runs to the Veeder counter.

The two-prism design that is used is made possible by the properties of the Wadsworth-Littrow mounting. In this mounting the radiation that passes through the exit slit has passed through the prism at minimum deviation. This means that the radiation is leaving the prism at the same angle at which it entered it. Accordingly, one may replace this prism by any other prism of a different material (provided that both prisms are isosceles) and all the mirrors will still be in line and in focus. The radiation passing through the exit slit will still be that which has passed through the prism at minimum deviation and the only difference will be that the radiation will be of a different wave-length. We have made use of this property in the following manner: The two Wadsworth mirrors have been accurately aligned so that when the table is rotated 180° M_5 is exactly where M_2 was and *vice versa*. This alignment was made by mounting the mirrors on a single casting which has a flat surface in a plane perpendicular to the top of the prism table and passing through the center of rotation. M_2 is held against the flat surface over a square opening and M_5 against a flat plate held against the flat surface of the casting with openings so that most of the surface of the mirror is exposed. There are two separate prism holders. The table is set in one of its two positions and C_3, P_1, M_3, M_4 and S_2 are adjusted so that the radiation entering S_2 is that which has passed through the prism at minimum deviation. This is done with the sodium D lines. The table is then rotated to the other position and it is only necessary to adjust P_2 so that radiation of the desired wave-lengths can reach S_2 within the possible rotation of the prism table (about 10°). There is no reason why this mounting cannot be

[1] We are indebted to the Globar Corporation for the gift of this item.

[2] This box was originally used as a double-walled air thermostat. The use of a thermostat was discontinued when it was found that the periodic fluctuations (±0.01°) of the thermostat at equilibrium were picked up by the thermopile.

extended to include as many prisms as one may wish. It takes only a few seconds to switch from the NaCl to the KBr prism or back again.

The concave mirrors are 5 cm in diameter with focal lengths about 33 cm. The face of the rocksalt prism is 4 cm×6 cm so that the effective aperture is a little less than $f:7$. For the KBr prism the aperture is not as favorable because the prism is only 4×4 cm. The mirrors are all arranged so as to minimize astigmatism.[3] The maximum angle between beams approaching and leaving the mirrors is 17°.

The receiver is a 26 junction Ag-Bi linear thermopile, constructed by Coblentz about 1915. While a more modern type of thermopile would probably increase the sensitivity and permit the use of narrower slits and thus increase the resolving power, the instrument as it stands seems to have enough resolving power for our purposes. It clearly resolves the ethylene bands at 1400 cm^{-1} into the envelopes of the P, Q and R branches.

The amplifying system is also shown in Fig. 1. It is similar to that described by Barnes, Brattain and Seitz,[4] except that N_1 and N_2 are Weston photronic cells which oppose each other. This eliminates errors due to fluctuations in the intensity of the light source. The part of the amplifying system enclosed in the solid frame is mounted on a concrete pier which is independent of the building. R is a portable light tight box which contains the paper moving mechanism. This is simply an old typewriter carriage and roller, with the original gear replaced by one three times as fine, so that the paper moves 1.2 mm for each notch of the ratchet. The ratchet is activated by a string from an eccentric on the same shaft as the devices that move the cell holders, shutter and table, which will be described below.

The type of recording system used is adapted from one described by Fahrentholz.[5] The prism table is moved one step at a time and while it is stationary the zero of the amplifying system, the intensity of the light source and the intensity of the transmitted radiation are recorded. The cell

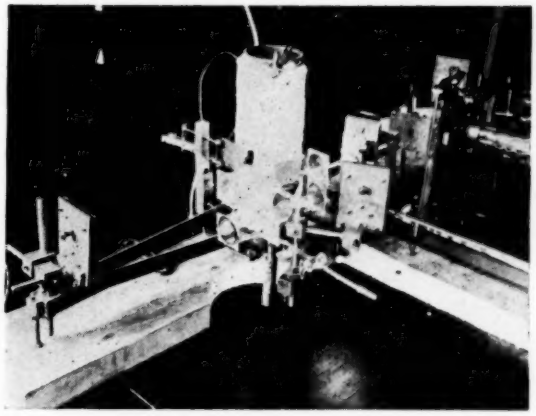

FIG. 2. Photograph of part of spectrograph.

holder is an aluminum casting and is mounted on the end of a piston which is raised by a cam. The photograph, Fig. 2, shows this and the rest of the optical train outside the spectrometer housing. When the piston rests on the circular quadrants of the cam the shutter is open and when it is rising or falling the shutter is closed. The cell holder supports two cells, one containing the substance under investigation, the other evacuated. When the piston is rising, the ratchet driving the table and that moving the photographic paper are moved one notch by means of eccentrics on the same shaft as the cam. This shaft turns at 2 r.p.m. through a 900–1 reduction box connected to an 1800 r.p.m. synchronous motor. The shutter is also moved by an eccentric which is geared to move twice as fast as the cam, so that it opens and closes twice in each cycle, recording the zero twice. The shutter is mounted so that it moves in front of the slit horizontally. Thus, even though it is moving continuously, the actual time of opening or closing is of very short duration compared to the time that it is open or closed. (The shutter moves through 5 cm, while the slit width is never greater than 1.5 mm.)

Figure 3 shows the kind of record that is made by this spectrometer. The records are easily measured by means of a simple device, shown in Fig. 4. A triangle with one side equal to 10 cm (and graduated in mm) has been marked on a transparent celluloid 30°–60°–90° triangle. A narrow strip of celluloid with a straight line ruled on it is pivoted so that the line rotates with the apex opposite to the ruled side of the tri-

[3] (a) Czerny and Turner, Zeits. f. Physik **61**, 792 (1930); (b) Czerny and Plettig, ibid. **63**, 590 (1930).
[4] Barnes, Brattain and Seitz, Phys. Rev. **48**, 582 (1935).
[5] Fahrentholz, Zeits. f. tech. Physik, 67 (1936).

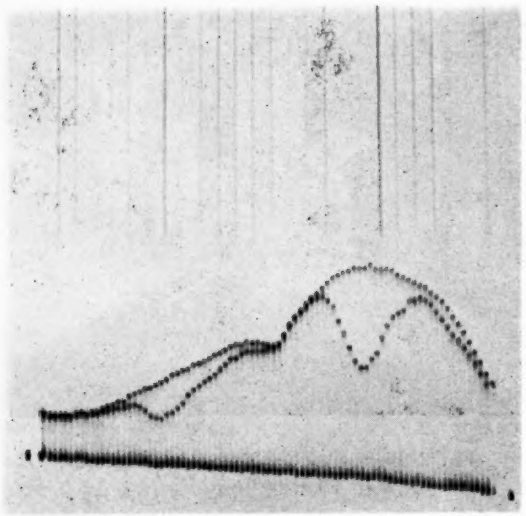

FIG. 3. A sample record (ethylene from 1650 to 5000 cm^{-1}) showing the CO_2 absorption of the atmosphere, the maximum of intensity of the source, and several ethylene bands.

angle as its center of rotation. If the instrument is placed so that the ruled edge is at the right parallel to the galvanometer deflections, the lower side of the triangle made to intersect the lowest point of a set, the upper side intersecting the highest point and the movable line set to intersect the middle point, then the intersection of this line with the ruled side will give the ratio of the smaller deflection to the larger one.[6]

This type of recording has many advantages over the usual continuous type. It eliminates uncertainties due to drift of the zero, change of intensity of the source of radiation and absorption by water vapor and carbon dioxide in the atmosphere. Such phenomena are indicated in Fig. 3. This discontinuous recording also eliminates any possibility of shifts in the recorded maxima due to time lag in the thermopile-recording system. It has the possible disadvantage that it takes more time to run through the spectrum, but this is, in our opinion, more than

[6] We are indebted to Dr. W. H. Avery for the design and construction of this measuring instrument.

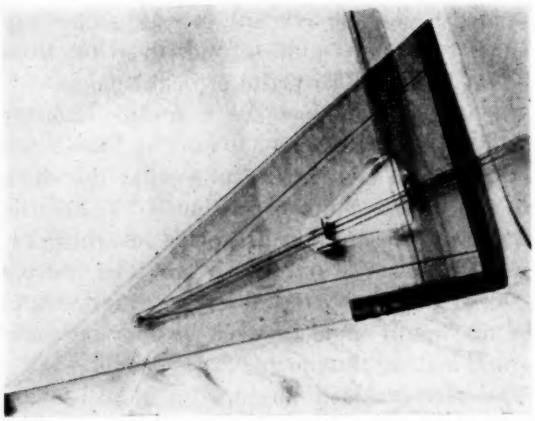

FIG. 4. Photograph of device for reading records.

compensated for by the added accuracy. To go from 3300 cm^{-1} to 700 cm^{-1} in steps of 3 Veeder numbers (this corresponds to about 30 cm^{-1} at 2000^{-1} and 3 cm^{-1} at 1000 cm^{-1}) takes about four hours and two feet of photographic paper. It takes only two or three minutes to change the instrument from automatic to hand recording by substituting a scale in place of R.

The rocksalt prism was calibrated empirically by means of the absorption bands of C_2H_4, C_2H_2, C_2H_6 and C_6H_6. The potassium bromide prism was also calibrated with these bands and the calibration extended to 400 cm^{-1} (25μ) by means of the known indices of refraction of KBr. While these indices are not known with great accuracy, the error introduced is less than 1 cm^{-1} at 500 cm^{-1}, due to the wide spread of the dispersion on a wave number scale.

The spectrometer table and screw were constructed by Mr. D. W. Mann of the physics department shop. We wish to acknowledge our gratitude to Professor D. C. Stockbarger of the Massachusetts Institute of Technology for the gift of several crystals of KBr and to Professor George B. Kistiakowsky for advice and encouragement. Part of this investigation has been supported by a grant from the Milton Fund of Harvard University.

Limits of Infra-Red Sensitizing*

G. KORNFELD
Eastman Kodak Research Laboratories, Rochester, New York
(Received January 26, 1938)

The competition between the thermal reaction and the photochemical reaction will set a natural limit to the extension of photographic methods into the infra-red region. From plausible assumptions concerning the velocity of the spontaneous reaction of molecules containing an excess of energy, it is concluded that this limit will be found at a wave-length of 2μ.

THE extension of photographic technique into the infra-red region can be extremely helpful in the investigation of vibrational bands, and for this purpose the passing of the long wave limit beyond its present value is very important. There does not seem any doubt that this end will be reached in the very near future, since the synthesis of the polymethine dyes, used as sensitizers, progresses steadily.[1] However, the polymethines are rather unstable substances, and their synthesis becomes increasingly difficult with their absorption spectrum shifting to longer wave-lengths. Thus, progress in this field is necessarily slow, since it has to fight against heavy odds.

It may be of some interest, therefore, to consider the theoretical boundaries of this progress—the limit which cannot be surpassed even by the ingenious methods of organic synthesis. Some years ago Czerny[2] pointed out that in the infra-red region space radiation increases rapidly with the wave-length. Calculating for different infra-red regions the number of quanta incident per cm^2 per second at room temperature, he found the number 4.0×10^{10} for the region between 1.5 and 2μ, and the number 2.4×10^{15} for the region between 3 and 4μ. The first number he showed to be equal to the infra-red radiation of the same region emitted by a Nernst burner at thirty meters distance, whereas the distance from the Nernst burner would have to be only twelve centimeters for the second number. It is doubtful whether the intensity in the first case would be sufficient to produce an appreciable density even during a long time—since the law of reciprocity is not valid for photographic exposure. There certainly can be no doubt, however, about the second case, so that the region between 3 and 4μ seems inaccessible for infra-red photography because of the competitive influence of thermal radiation.

Besides the thermal radiation, however, there is yet another possibility, also mentioned by Czerny: the reaction of molecules to which an energy corresponding to infra-red radiation has been imparted in thermal equilibrium. It remains to be seen whether the limit of infra-red sensitizing will not be shifted even nearer to shorter wave-lengths by this reaction than by the influence of space radiation. To answer the question, the velocity of this reaction must be compared with the reaction velocity produced by exposure.

To arrive at this last value it will be assumed that a developable image is obtained after an exposure of a few seconds, so that the plate would already show an appreciable density if exposed to the same radiation for one second. By using the data which Leszynski[3] obtained for exposure of a sensitized plate, the rate of the corresponding primary reaction can be determined. He found that of 150 quanta one was absorbed, and the number of incident quanta per cm^2 per second (using an energy of 2.5 *HK*) could be determined by this formula (p. 266) to be 9×10^{14}, so that $6\times10^{12}=10^{12.8}$ *quanta* were absorbed per cm^2 per second. This actually is the velocity which, according to the assumption, produces a developable density on the plate in one second. It is further assumed that the same number of quanta would be necessary in the

* Communication No. 657 from the Kodak Research Laboratories.

[1] L. G. S. Brooker and G. H. Keyes, J. Frank. Inst. **219**, 255 (1935); W. Dieterle and O. Riester, Zeits. f. wiss. Phot. **36**, 68, 141 (1937).

[2] M. Czerny, Zeits. f. Physik **53**, 1 (1929).

[3] W. Leszynski, Zeits. f. wiss. Phot. **24**, 261 (1927).

infra-red region, which means that the absorption of the sensitizers for their specific regions is taken to be equal, as a first approximation. (This assumption may be wrong by an order of ten, especially as the increase of quanta per energy unit has not been taken into account.)

The velocity of the thermal reaction, on the other hand, can be calculated from the following expression:

$$10^{-Q/4.57T} \cdot v \cdot t \cdot n,$$

where Q is the energy of the quantum in question, expressed in calories, T, the absolute temperature, v, the velocity of the spontaneous reaction, t, the time in seconds, and n, the number of sensitizer molecules per cm² surface. The value Q varies according to the frequency, T is taken to be room temperature (300° abs.), and n is supposed to be 10^{14} for optimum sensitizing, according to Leermakers, Carroll and Staud.[4]

The velocity of the spontaneous reaction, v, remains to be found. In an early paper, Polanyi and Wigner[5] had assumed that a molecule containing a certain surplus amount of energy would need 10^{-13} seconds for concentrating this energy on a single bond where it could be used as critical activation energy. This rule was found to hold good in many cases, although some exceptions have been pointed out since that time. In a recent paper H. Sachsse[6] expressed the opinion that this time might be much longer for large molecules, and there is a special reason, moreover, to assume this time to be longer in this case—of the order of 10^{-7} to 10^{-8} seconds: the electronic state of the sensitizing dye is changed in the primary reaction, and for this change the energy transfer will be less easy than for the change in a vibrational bond. Volmer and Froehlich[7] found the unusually large value of 2×10^{-8} seconds for the predissociation of N_2O, and G. Herzberg[8] showed that for this molecule predissociation occurred by the crossing of two electronic states.

On inserting the various values for v in the formula given above, it becomes obvious that the value $v=10^{-13}$ sec.$^{-1}$ is much too large. For, if the formula is applied to the wave-length 1.356μ, the limit which actually has been reached so far in infra-red photography, the velocity of the thermal reaction (the corresponding value for Q being 20970 cal.) turns out to be

$$10^{-15.3}\times10^{13}\times10^{14}=10^{11.7}$$

reacting molecules per second, only ten times less than the velocity obtained by exposure. This means that within ten seconds of contact with the sensitizer the plate should already obtain an appreciable developable density—which would make it utterly useless for practical purposes. But with $v=10^{7}$ sec.$^{-1}$, the velocity is

$$10^{-15.3}\times10^{7}\times10^{14}=10^{5.7}$$

reacting molecules per second, which corresponds to such a small intensity of exposure that, even with an assumed reciprocity law, the plate would only be affected after a few months; according to the reciprocity law failure, however, no effect should be expected at all.

In the same way the expression for 1.5μ is found to be

$$10^{-13.8}\times10^{7}\times10^{14}=10^{7.2}$$

reacting molecules per second, which is the $10^{5.6}$ part of the velocity obtained by exposure. Again the reciprocity law failure makes any effect improbable.

For 2.0μ, however, with $Q=14210$ cal., the thermal velocity will be

$$10^{-10.0}\times10^{7}\times10^{14}=10^{11}$$

reacting molecules per second, so that within one or two minutes the plate should be affected.

According to this reasoning, infra-red sensitizing should be impractical even at 2μ where space radiation does not seriously interfere. At slightly shorter wave-lengths, with the plates kept in solid carbon dioxide most of the time, exposure might be used to give a solarized image. The only possibility left for efficient sensitizing at $\lambda=2\mu$ and at longer wave-lengths would lie in the existence of dyes with a spontaneous reaction velocity much smaller than 10^{7} sec.$^{-1}$. This, however, seems very improbable.

[4] J. A. Leermakers, B. H. Carroll and C. J. Staud, J. Chem. Phys. **5**, 878 (1937).
[5] M. Polanyi and F. Wigner, Zeits. f. physik. Chemie **A139**, 439 (1928).
[6] H. Sachsse, Zeits. f. physik. Chemie **B32**, 87 (1936).
[7] M. Volmer and H. Froehlich, Zeits. f. physik. Chemie **B19**, 85 (1932).
[8] G. Herzberg, Zeits. f. physik. Chemie **B17**, 68 (1932).

The Fine Structure of the Totally Symmetrical Raman Lines in Benzene and Benzene-d_6

A. LANGSETH AND R. C. LORD, JR.*
Universitetets kemiske Laboratorium, Copenhagen, Denmark
(Received February 10, 1938)

IN a forthcoming article[1] on the Raman spectra of the deuterated benzenes, we discuss, *inter alia*, the problem of the origins of the four satellites of the 992 cm^{-1} Raman line in benzene. In view of the recent paper of Cheng, Hsueh and Wu[2] on the origin of one of these satellites, it is perhaps not amiss to give in this place a separate and briefer discussion of the question.

Let us state immediately our interpretation of these lines. Two of the components (denoted I and IV) are due to transitions from the first excited state of the E_g^+ vibration ν_6 to the two levels of the resonance doublet $E_g^+ : A_{1g}+E_g^+$ ($\nu_8 \backsimeq \nu_1+\nu_6$). The other two (II and V) are two totally symmetrical lines of the molecule $C_5{}^{12}C^{13}H_6$ derived from the frequencies ν_1 and ν_{12} in benzene. Quantitative predictions of the frequency and intensity of the satellites on the basis of this interpretation agree satisfactorily with the experimental data.

The positions of components I and IV can be calculated quite accurately from the differences in the observed frequencies of ν_6 and the resonance doublet. Using the data of Klit and Langseth[3] for the sake of consistency with later comparisons, we find $\tilde{\nu}_I = 1585.9-606.4 = 979.5$ cm^{-1}; $\tilde{\nu}_{IV} = 1604.2-606.4 = 997.8$ cm^{-1}. The sum of the intensities of I and IV should be given very closely by the product of the intensity of the main line, due to ν_1 (hereafter denoted by III), and the appropriate Boltzmann factor, namely $2\times\exp(-hc\tilde{\nu}_6/kT)$. The ratio of intensities, I_I/I_{IV}, should be the same as the ratio of the intensity of the *upper* component of the resonance doublet ($\tilde{\nu}=1604.2$) to that of the lower ($\tilde{\nu}=1585.9$), if one makes the assumption that polarizability change due to second order tones is negligible in comparison with that due to allowed fundamentals. The ratio is 0.84.[4] Therefore the ratios I_I/I_{III} and I_{IV}/I_{III} should be 0.051 and 0.059, respectively, at room temperature.

Satellite II was first ascribed to $C_5{}^{12}C^{13}H_6$ by Gerlach.[5] His interpretation has been accepted by Cheng, Hsueh and Wu,[2] and on its basis they have calculated (by a perturbation method) that the frequency difference between II and III should be 6.3 cm^{-1}. This agrees closely with the shift of 6.2 cm^{-1} which one may compute in a simpler fashion (by calculating ν_1 for the hypothetical molecule $C_6{}^{12.167}H_6$, which should have the same value[6] as ν_1 in $C_5{}^{12}C^{13}H_6$). It does *not* agree, however, with the observed frequency shift, which, according to measurements made by one of us (A. L.), is 8.7 cm^{-1}.[7] The disagreement, which is beyond the limits of experimental error, may be attributed to the circumstance that the approximations which make calculation of the shift possible are not strictly valid because of the presence of a fundamental frequency, ν_{12}, in the immediate vicinity of ν_1. ν_{12} lies at about 1010 cm^{-1} in benzene[8] and should shift to *ca.* 1003 cm^{-1} in $C_5{}^{12}C^{13}H_6$.

If interaction between ν_1 and ν_{12} causes the observed depression of ν_1 by 2.4 cm^{-1} in $C_5{}^{12}C^{13}H_6$, ν_{12} should be raised by a like amount. A more noticeable result of the interaction should be the donation of Raman intensity to ν_{12}, thus enabling it to appear as a satellite (V) of ν_1 in benzene. The amount of intensity transferred from ν_1 to ν_{12} because of resonance interaction may be calculated in the usual fashion.[9] The intensity ratio of V to II will be:

$$I_V/I_{II} = (W-\Delta)/(W+\Delta). \qquad (1)$$

Here W is the actual frequency difference

* National Research Council Fellow.
[1] Langseth and Lord, Kgl. Danske Vids. Selsk., Math.-fys. Medd. XVI (1938).
[2] Cheng, Hsueh and Wu, J. Chem. Phys. **6**, 8 (1938).
[3] Klit and Langseth, Nature **135**, 956 (1935).
[4] Angus, Ingold and Leckie, J. Chem. Soc. London 929 (1936).
[5] Gerlach, Sitz. Math.-Nat. Bayer. Akad. München, 39 (1932).
[6] Cf. Teller, *Hand und Jahrbuch der chemische Physik*, Vol. 9, pp. 142 ff.
[7] In reference 2 the observed value of the shift appears to be 8.2 cm^{-1} from the accurate frequency values printed at the top of Fig. 1.
[8] Klit and Langseth, J. Chem. Phys. **5**, 925 (1937).
[9] See Placzek, *Handbuch der Radiologie*, Vol. 7, Part 2, p. 321.

between V and II, and Δ is the value this difference would have if there were no interaction between ν_1 and ν_{12}. $(W-\Delta)$ is therefore the increased separation of ν_1 from ν_{12} due to interaction, namely 2×2.4, or 4.8 cm^{-1}. From this value of $(W-\Delta)$ and the observed value of W (21.7 cm^{-1}), the ratio (1) is found to be 0.12. The total intensity of II and V should be very nearly that of III save for the rarity of $C_5{}^{12}C^{13}H_6$ molecules. There are about six of the latter in every hundred molecules of benzene. Therefore $I_{II}/I_{III}=0.0536$, and $I_V/I_{III}=0.0064$.

The foregoing frequencies and intensities have been assembled in Table I together with unpublished experimental data obtained by one of us (A. L.) in 1931, and with the frequencies given by Angus, Ingold and Leckie[4] in their summary of the Raman data on benzene. The observed intensities in column 5 are visual estimates (made in 1931) and are not to be considered of more than semi-quantitative significance. The fact remains, however, that component I is decidedly less intense than II, although the calculation assigns them almost equal intensity. This discrepancy is perhaps due to neglect of the effect of second-order polarizability changes in computing I_I/I_{IV}. With this one exception, the interpretation fits the observed facts very well. The methods we have used to compute intensity ratios lead also to the conclusion that all the satellites should have the same depolarization factor as ν_1, namely $\rho=0.09$. This agrees at least qualitatively with reference 2, which sets an upper limit, $\rho=0.4$, for component II.

The fine structure expected for ν_1 in benzene-d_6 is simpler than that in benzene. ν_8 appears in benzene-d_6 as a single line only, and therefore a satellite due to $\nu_8-\nu_6$ should be lacking, since

TABLE I. *Fine structure of ν_1 in benzene.*

Frequency of Components in cm^{-1}				Intensity of Components		
	Observed			Observed		
No.	Langseth	Summary[4]	Calc.	Langseth	Ref. 2	Calc.
I	979.6	979	979.5	5	—	5.1
II	983.8	984	986.2	10	6	5.4
III	992.5	992	(992.5)	100	100	(100)
IV	997.9	999	997.8	10	—	5.9
V	1005.5	1005	ca. 1003	1	—	0.6

TABLE II. *Fine structure of ν_1 in benzene-d_6.*

Frequency of Components in cm^{-1}		Intensity of Components	
No.	Observed	Calculated	Observed	Calculated
I	939.5	940.2	10	5.8
II	945.2	(945.2)	(100)	(100)
III	962.1	ca. 960	0.1	0.2

the product of the Boltzmann factor (0.1) and the intensity expected of combination tones (<0.01) is overwhelmingly small. The component $(\nu_1+\nu_6)-\nu_6$ should coincide with ν_1.

The calculated shift of ν_1 in $C_5{}^{12}C^{13}D_6$ is 5.0 cm^{-1}, and the observed one 5.7. Here the difference is more readily ascribable to experimental error than in benzene, but if we attribute all of it to interaction with ν_{12}, we may compute the intensity ratio of ν_{12} to ν_1 in $C_5{}^{12}C^{13}D_6$ as 0.03, i.e. ν_{12} should have only about $\frac{1}{4}$ the relative intensity of satellite V in benzene. ν_{12} should be higher than ν_1 by very nearly the same amount as in benzene, and therefore should lie in the neighborhood of 960 cm^{-1}. Actually there is an extremely faint line at 962 cm^{-1}, but its assignment is not entirely conclusive, because it is known[8] that both ortho- and parabenzene-d_4 have their strongest lines at this point (at 960.0 ± 0.4 cm^{-1}) and it is conceivable that the extended exposures which revealed the line may have been able to record the benzene-d_4 frequencies even though their total concentration was probably less than 0.02 percent. That the line may actually be ν_{12} is given some support by the failure to observe the strongest frequency of metabenzene-d_4 at 954 cm^{-1}. This frequency should appear with not less than half the intensity of the 962 line if the latter is really due to the other benzene-d_4's.

The fine structure data on benzene-d_6, hitherto unpublished, are summarized in Table II. Not included in the table are two very faint lines, observed at 950.7 and 977.3 cm^{-1}, which belong to benzene-d_5,[8] and which are not to be expected in hydrogen-free benzene-d_6. The latter of these lines has also been reported by Angus, Ingold and Leckie.[4] The difference tone $\nu_8-\nu_6$ should lie in this neighborhood (at *ca.* 975 cm^{-1}), but, for reasons just given, should not be expected to make its appearance.

Determination of Intermolecular Forces from the Joule-Thomson Coefficients

J. O. HIRSCHFELDER, R. B. EWELL AND J. R. ROEBUCK
Departments of Chemistry and Physics, University of Wisconsin, Madison, Wisconsin

(Received February 2, 1938)

The energy of interaction between nonpolar molecules is determined inductively from a study of the experimental Joule-Thomson coefficients. These coefficients have been measured very accurately for some substances, and in these cases our method of analysis is preferable to other methods which utilize less accurate data. It follows from classical statistical mechanics that:

$$\mu_0=(-2\pi N/C_p^0)\times\int_0^\infty r^2[1-(1-E(r)/kT)\exp(-E(r)/kT)]dr.$$

Here μ_0 and C_p^0 are the Joule-Thomson coefficient and specific heat at constant pressure, respectively, both extrapolated to zero pressure; N is Avogadro's number; k is Boltzmann's constant; and $E(r)$ is the energy of interaction of two molecules separated by a distance r. This integral is evaluated using the Lennard-Jones form for the potential energy, $E(r)=-cr^{-6}+lr^{-s}$. Here c, l, and s are varied so as to give the best agreement with the experimental μ_0. The numerical tables required for these analyses are given. Helium and argon are studied in detail. The necessary quantum corrections are made for helium and shown to be negligible for argon. The Joule-Thomson studies of Roebuck and Osterberg are found to be in accord with other PVT measurements. It is shown that all substances having a mutual potential energy of the Lennard-Jones form with the same value for s, satisfy the theorem of corresponding states. Consequently, at low pressures, the Boyle point, T_B, is proportional to the Joule-Thomson inversion point, T_I, and $T_B=0.532T_I$. This relationship is verified in the case of N_2.

I. INTRODUCTION

THE interaction between the individual molecules of a substance is evidenced by a variety of physical and chemical properties such as the deviations from the ideal gas laws, the behaviour of liquids and crystals, the solubilities and tendencies for adsorption, etc. The investigation of any of these properties should be useful in determining the forces of attraction and repulsion between the molecules. Lennard-Jones[1] has been successful in analyzing these forces through a study of the experimental second virial coefficients. In this paper we extend his methods to utilize the accurate data which are available for the Joule-Thomson coefficients. A formulation based on statistical mechanics gives an explicit relationship between the Joule-Thomson coefficients and the energy of interaction between the molecules. This energy of interaction may be expressed in the form:

$$E(r)=-c/r^6+l/r^s \qquad (1)$$

as a compromise between accuracy of representation and tractability in use. Here $E(r)$ is a function of the separation between the molecules, r, but not a function of the temperature. c, l, and s are parameters which are adjusted so as to obtain the best fit with the experimental data. In this paper, we give a detailed comparison of the experimental Joule-Thomson coefficients for helium and argon with the theoretical formulation and present numerical tables which will aid in making similar analyses for other substances. The calculated and the experimental Joule-Thomson coefficients should agree if the function corresponds to the true interaction energy, but other functions may exist which would fit the data equally well. Quantum mechanics may be used to decide which are the more reasonable ones. The statistical formulae must be corrected to take into account the nonclassical interactions between the molecules. These corrections are sometimes appreciable as in the case of helium at low temperatures. For heavier molecules at reasonably high temperatures these corrections are negligible. In such cases we might expect the theorem of corresponding states to apply, and the properties of one gas would be simply related to those of another gas. This theorem is valid if the potential energy between a pair of molecules can be expressed in the form:

$$E(r)=E_0f(r/r_0),$$

where E_0 and r_0 are characteristic constants of the molecules, and $f(r/r_0)$ is a universal function.

[1] Lennard-Jones, Chapter X of Fowler's *Statistical Mechanics* (Cambridge University Press, 1936), and more recently, Physica **4**, 941 (1937).

The potential energy of Eq. (1) is of this form if s is supposed to have the same value for all substances under consideration.

II. Relations between the Joule-Thomson, the Free Expansion, and the Virial Coefficients

The imperfection of a gas is due to the attractions and repulsions of the molecules. Both the Joule-Thomson and the virial coefficients are direct measures of these forces and both become zero for a perfect gas. There are a number of ways of defining the virial coefficients,[2] but for the purposes of this paper we shall use the form of the equation of state:

$$pV=RT(1+Bp+Cp^2+Dp^3+\cdots). \quad (2)$$

Here B, C, D, $\cdots$ are called the second, third, fourth, $\cdots$ virial coefficients and are functions of the temperature but not of the pressure. In this equation, p is the pressure in atmospheres, T is the absolute temperature, V is the molal volume in cm^3, and R is the gas constant per mole, i.e. $R=82.07$. It is easy to show that these virial coefficients are related to the Joule-Thomson coefficient,

$$\mu\equiv(\partial T/\partial p)_H \quad (3)$$

where H is the enthalpy or heat content of the gas. From thermodynamics[3] it may be shown that

$$\mu=-(\partial H/\partial p)_T/C_p \quad (4)$$

where C_p is the specific heat at constant pressure. But since

$$(\partial H/\partial p)_T=V-T(\partial V/\partial T)_p \\ =-T^2[(\partial/\partial T)(V/T)]_p \quad (5)$$

it follows that

$$\mu=T^2[(\partial/\partial T)(V/T)]_p/C_p. \quad (6)$$

Both the numerator and the denominator of (6) may be expressed in terms of the virial coefficients. By integrating the relation $V=(\partial F/\partial p)_T$, with respect to pressure where F is the free energy (or thermodynamic potential) and using Eq. (2), we obtain

$$F=F^0+RT\log p+RTBp+(1/2)RTCp^2 \\ +(1/3)RTDp^3+\cdots. \quad (7)$$

Here F^0 is the constant of integration which is a function of temperature but not of pressure.[4] Since $C_p=-T(\partial^2F/\partial T^2)_p$, it follows from (7) that

$$C_p=C_p^0-RT\left[p\frac{d^2(BT)}{dT^2}+(1/2)p^2\frac{d^2(CT)}{dT^2} \right. \\ \left. +(1/3)p^3\frac{d^2(DT)}{dT^2}+\cdots\right], \quad (8)$$

where C_p^0 is the specific heat at zero pressure. In terms of C_v^0, the specific heat at constant volume for infinite volume, $C_p^0=C_v^0+R$. In cases where neither C_p^0 nor C_v^0 can be obtained directly from experimental measurements with sufficient accuracy, it is often convenient to make use of spectroscopic information by means of the equation:[5]

$$C_v^0=R[(\partial/\partial T)T^2(\partial/\partial T)(\log f)]_v, \quad (9)$$

where f is the partition function for the molecule, or the sum of all of the quantum states each multiplied by its Boltzmann factor, i.e., expo-

[2] Virial coefficients are defined in the literature according to the three equations of state: (1). as from Eq. (2). (2). the equation $pV=A_p+B_pp+C_pp^2+\cdots(2')$. Here it is obvious that $A_p=RT$ and that B_p, $C_p\cdots$ are equal to RT times our B, C, $\cdots$ respectively. (3). the equation of state given in powers of $1/V$, $pV=A_v+B_v/V+C_v/V^2+\cdots(2'')$. Here again $A_v=RT$ but the relationship of the higher virials to our B, $C\cdots$ are not so obvious. To find these relations it is necessary to substitute for $1/V$ in $(2'')$ $1/V=p(RT)^{-1}(1+Bp+Cp^2+\cdots)^{-1}$ from Eq. (2), expand the right-hand side of the equation in powers of p, and equate the coefficients in this expansion to the corresponding virial coefficients of Eq. (1). Thus we find

$$B=B_v/R^2T^2, \quad C=C_v/R^3T^3-B_v^2/R^4T^4, \\ D=D_v/R^4T^4-3C_vB_v/R^5T^5+2B_v^3/R^6T^6.$$

The value of R which is used by different workers is another source of confusion. In theoretical treatments it is customary to express R in molal units whereas experimental workers prefer to express R so that $pV=1$ at unit pressure and 0°C. The conversion of R from these experimental to the molal units then involves the use of all of the virial coefficients. Kammerlingh-Onnes and his coworkers at Leiden have adopted the international atmosphere as their unit of pressure. Holborn and Otto and their colleagues at Berlin have adopted 1 meter of mercury $=1000/760$ atmos. as their unit of pressure. In this country, the Amagat units have become popular. Here the int. atm. is the unit of pressure, as in the Leiden units, but the unit of density is the density of nitrogen at 0°C and 1 atmos. (1.2506 grams per liter).

[3] See for example Lewis and Randall, *Thermodynamics* (McGraw-Hill 1923), pp. 68, 162 and 163.

[4] The super- or subscript, zero, is used throughout this paper to denote the value of the quantities at zero pressure.

[5] Fowler, *Statistical Mechanics*, second edition (1936), p. 197, Eq. (611).

nential of minus the energy of the state divided by kT. At reasonably high temperatures C_v^0 usually does not deviate appreciably from its classical value of $(3/2)R$ for monatomic molecules, $(5/2)R$ for diatomic, etc. At very low temperatures, quantum effects occur and at very high temperatures for di- and polyatomic molecules, the specific heat of internal vibrations appears, but even in these cases the evaluation of C_v^0 to the desired accuracy should not be the source of any great amount of difficulty. The numerator of Eq. (6) is readily obtained from (1) so that we finally derive the Joule-Thomson coefficient in terms of the virial coefficients

$$\mu=\frac{RT^2[dB/dT+pdC/dT+p^2dD/dT+\cdots]}{C_p^0-RT\left[p\frac{d^2(BT)}{dT^2}+(1/2)p^2\frac{d^2(CT)}{dT^2}+(1/3)p^3\frac{d^2(DT)}{dT^2}+\cdots\right]}. \tag{10}$$

For the purpose of making our analysis, it is more convenient to expand the right side of Eq. (10) in a Maclaurin series in powers of pressure so that

$$\mu=\mu_0+p(\partial\mu/\partial p)^0_T+(1/2)p^2(\partial^2\mu/\partial p^2)^0_T+\cdots, \tag{11}$$

where μ_0 is the Joule-Thomson coefficient extrapolated to zero pressure $(\partial\mu/\partial p)^0_T$ is its derivative with pressure at constant temperature evaluated at zero pressure, and $(\partial^2\mu/\partial p^2)^0_T$ is its corresponding curvature at zero pressure. Here

$$\mu_0=\frac{R}{C_p^0}T^2\frac{dB}{dT} \tag{12}$$

an equation similar to that obtained by Whitelaw.[6] This relation is particularly useful because it enables us to determine the second virial coefficient regardless of the magnitude of the third, fourth, etc. virials. Similarly

$$\left(\frac{\partial\mu}{\partial p}\right)^0_T=\frac{RT}{C_p^0}\left[T\frac{dC}{dT}+\mu_0\frac{d^2(BT)}{dT^2}\right] \tag{13}$$

and

$$\left(\frac{\partial^2\mu}{\partial p^2}\right)^0_T=\frac{RT}{C_p^0}\left[2T\frac{dD}{dT}+\mu_0\frac{d^2(CT)}{dT^2}+2\left(\frac{\partial\mu}{\partial p}\right)^0_T\frac{d^2(BT)}{dT^2}\right]. \tag{14}$$

Most of our analysis will be concerned with the second virial coefficient and with μ_0. Later we shall use Eq. (13) to show how the potential energy between pairs of molecules, leads to approximately the correct pressure dependence of the Joule-Thomson coefficient when we obtain the potential from a study of μ_0 as a function of temperature.

If μ_0 is known as a function of temperature, we can integrate Eq. (12) to obtain the second virial coefficient except for a constant of integration:

$$B=\int_{T_0}^{T}(C_p^0\mu_0/RT^2)dT+(B)_{T_0}. \tag{15}$$

Here T_0 is any convenient temperature. Whitelaw used this equation to show that the data of Roebuck and Osterberg for the Joule-Thomson coefficients of helium were consistent with the second virial coefficients determined by other workers. The constant of integration of Eq. (15) could be evaluated on the reasonable supposition that as the temperature becomes infinite, B approaches zero. But unfortunately the temperatures at which the Joule-Thomson effect have been studied are not sufficiently high to make such an extrapolation accurate. We shall therefore resort to an indirect method of obtaining this constant. First we use the Joule-Thomson coefficient to determine the interaction energy between a pair of molecules. Then substituting this mutual potential energy expression into the statistical mechanical formula for B, Eq. (19), we obtain the absolute value of the second virial coefficient at any temperature. Because statistical mechanics is developed in terms of molecular models, it is often capable of giving more information from the same data than could be obtained from thermodynamics alone. As a matter of fact we will show that using a rather good form for the potential energy, the Boyle point at low pressures is 0.532 times the temperature of inversion of the Joule-

[6] Whitelaw, Physica 1, 749 (1934).

Thomson effect. When T_0 is taken to be the Boyle point, the constant of integration in Eq. (15) is $(B)_{T_0}=0$.

The coefficient of free expansion, $\eta\equiv(\partial T/\partial p)_U$ where U is the internal energy of the gas, is another thermodynamical property closely related to the Joule-Thomson coefficient. Roebuck[7] has shown that

$$\eta=\frac{\mu C_p+[(\partial/\partial p)(pV)]_T}{C_p-[(\partial/\partial T)(pV)]_p}. \tag{16}$$

Using Eqs. (2), (8) and (10) it is easy to show that this is equivalent to the relation:

$$\eta=\frac{\mu_0 C_p^0+RTB+pR(d(CT^2)/dT)+p^2(R/T)(d(DT^3)/dT)+\cdots}{C_v^0-Rp(d/dT)T(d(BT)/dT)-(1/2)(Rp^2/T)(d/dT)T^2(d(CT)/dT)+\cdots}. \tag{17}$$

And the coefficient of free expansion extrapolated to zero pressure has the simple form:

$$\eta_0=\frac{\mu_0 C_p^0}{C_v^0}+\frac{RTB}{C_v^0}=\frac{RT}{C_v^0}\frac{d(BT)}{dT}. \tag{18}$$

III. Relations between the Thermodynamic Properties and the Intermolecular Energy

Fowler[8] and others have shown that, if the molecules in the gas interact as one would expect on the basis of classical mechanics, the second virial coefficient is related to the energy of interaction of a pair of molecules $E(r)$ in the following way:

$$B=\frac{2\pi N}{RT}\int_0^\infty r^2[1-\exp(-E(r)/kT)]dr, \tag{19}$$

where r is the separation between a pair of molecules, k is Boltzmann's constant and N is Avogadro's number. Substituting this expression for B into Eq. (12), we find that the Joule-Thomson coefficient extrapolated to zero pressure is

$$\mu_0=\frac{-2\pi N}{R}\left(\frac{R}{C_p^0}\right)$$
$$\times\int_0^\infty r^2\left[1-\left(1-\frac{E(r)}{kT}\right)\exp\left(-\frac{E(r)}{kT}\right)\right]dr. \tag{20}$$

Since C_p^0 and C_v^0 are usually expressed in units of the gas constant R, it is convenient to retain the ratios $\left(\frac{R}{C_p^0}\right)$ and $\left(\frac{R}{C_v^0}\right)$ in the formulae. Similarly from (19) and (18), the coefficient of free expansion extrapolated to zero pressure is

$$\eta_0=-\frac{2\pi N}{R}\left(\frac{R}{C_v^0}\right)\int_0^\infty r^2\frac{E(r)}{kT}\exp\left(-\frac{E(r)}{kT}\right)dr. \tag{21}$$

These equations permit us to determine $E(r)$ inductively if we know the experimental values of B, μ_0, or η_0 at different temperatures. Conversely, if we know the energy of interaction $E(r)$ either from theoretical or other experimental considerations, they permit us to calculate the thermodynamic properties of the substance. Lennard-Jones[9] has confined his analysis to a study of B whereas we find it equally as convenient to study μ_0 for which very accurate experimental data are available.

Before introducing any complicated expressions for the potential energy it is instructive to examine the gross properties of the second virial, Joule-Thomson, and free expansion coefficients. For this purpose we introduce a simple potential energy function which contains the essential features. Such a function is one first used by Herzfeld and Goeppert-Mayer.[10] Here, as shown in Fig. 1,

$E(r)=\infty$	when	r is less than r_0,
$E(r)=-D$		r lies between r_0 and r_a,
$E(r)=0$		r is greater than r_a.

When this function is inserted into Eqs. (19),

[7] Roebuck, Proc. Am. Acad. Sci. **64**, 287 (1930).

[8] R. H. Fowler, *Statistical Mechanics*, second edition (Cambridge Press, 1936) Chapter 8; Proc. Camb. Phil. Soc. **22**, 861 (1925). Also Ursell, Proc. Camb. Phil. Soc. **23**, 685 (1927).

[9] Lennard-Jones, Chapter X of Fowler's *Statistical Mechanics* (1936) and more recently, Physica **4**, 941 (1937).

[10] Herzfeld and Goeppert-Mayer, Phys. Rev. **46**, 995 (1934).

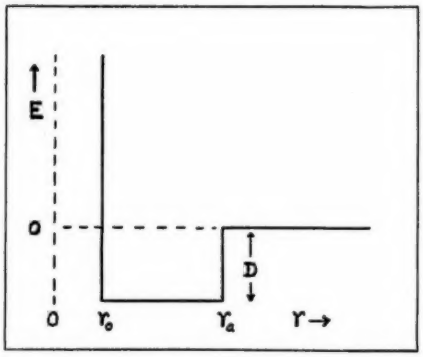

FIG. 1. The energy of interaction, E, as a function of the internuclear separation, r, for idealized molecules. This function was used by Herzfeld and Goeppert-Mayer.

(20) and (21), we obtain:

$$B=\frac{2\pi N}{3RT}r_0^3\left[1-\frac{r_a^3-r_0^3}{r_0^3}\{\exp(D/kT)-1\}\right]. \quad (22)$$

$$\mu_0=\frac{-2\pi N}{3R}\left(\frac{R}{C_p^0}\right)r_0^3\left[1-\frac{r_a^3-r_0^3}{r_0^3}\times\left\{\left(1+\frac{D}{kT}\right)\exp(D/kT)-1\right\}\right], \quad (23)$$

$$\eta_0=\frac{2\pi N}{3R}\left(\frac{R}{C_v^0}\right)r_0^3\times\left[\left(\frac{r_a^3-r_0^3}{r_0^3}\right)\frac{D}{kT}\exp(D/kT)\right]. \quad (24)$$

Here we see that B, μ_0, and η_0 are all proportional to the cube of the collision diameter, r_0. At low temperatures, the exponential term due to the attraction between the molecules, D, is of paramount importance, whilst at high temperatures it approaches unity. At high temperatures, B and μ_0 are only slightly affected by the attraction between the molecules and the limiting values are the same as for rigid spheres. The free expansion, η_0, seems to be very sensitive to the exact form for the potential energy for even at high temperatures it involves a characteristic of the attractive part of the potential, $(r_a^3-r_0^3)D$. From (24) it seems that η_0 could never be negative, and this assertion is made in a number of the texts. However, as evidence of the sensitivity of the free expansion to the potential function, it may be cited that this conclusion is not borne out when a more accurate potential is used. As a matter of fact Roebuck and Osterberg[11] have found that for helium it is actually negative at high temperatures.

As Wigner[12] and Slater[13] have pointed out, quantum-mechanical interactions between the molecules in the gas will introduce two types of corrections to the classical virial coefficient of Eq. (19). The first correction is due to the Pauli exclusion principle which requires that two similar molecules interacting must obey either the Bose-Einstein or the Fermi-Dirac statistics. The use of these statistics is well known in the case where the molecules are like atoms, and their interaction results in the formation of an ortho or para diatomic molecule. Just as in this case, the Bose, Fermi, and classical statistics lead to the same distributions when the thermal energy, kT, becomes large compared with the separation between the energy levels of rotation of the two molecules as a unit. Gropper[14] and recently Beth and Uhlenbeck[15] have considered this effect, and they were able to show that this correction is negligible except for the lightest molecules at the lowest temperatures. The second quantum-mechanical effect, however, leads to corrections which are sufficiently large to warrant consideration in any critical study of the properties of gases. It is due to the formation of double molecules when the relative kinetic energy of the colliding molecules is less than the potential energy of their attraction. The double molecules, just like diatomic species, possess discrete rotational and vibrational states for their relative motions and therefore have quite a different energy distribution from what one would expect classically. Uhlenbeck and Beth[16] have developed the correction terms to the second virial theorem so that we are able to correct the error due to this cause. According to Uhlenbeck and Beth:

$$B=B_{\text{class}}+B_q+\cdots, \quad (25)$$

where B_{class} is the B of Eq. (19) and B_q is the quantum-mechanical correction involving the

[11] Roebuck and Osterberg, Phys. Rev. **45**, 332 (1934).
[12] E. Wigner, Phys. Rev. **40**, 749 (1932).
[13] J. C. Slater, Phys. Rev. **38**, 237 (1931).
[14] Gropper, Phys. Rev. **50**, 963 (1936); **51**, 1108 (1937).
[15] Beth and Uhlenbeck, Physica **4**, 915 (1937).
[16] Uhlenbeck and Beth, Physica **3**, 729 (1936).

lowest power of h. The series converges rapidly for high temperatures and therefore it will suffice to consider B_q:

$$B_q=\frac{N^2h^2}{24\pi RMk^3T^4}\int_0^\infty r^2\left(\frac{\partial E}{\partial r}\right)^2 e^{-E(r)/kT}dr. \quad (26)$$

Here h is Planck's constant and M is the molecular weight of the gas. The absolute magnitude of this correction for helium and argon at various temperatures will be discussed in a later section.

The second virial coefficients for two isotopic molecules provide a direct measurement of the quantum correction. For this case $E(r)$ and hence B_{class} is the same for the two molecules, but the quantum correction according to Eq. (26) involves the mass as well as the potential energy of the molecules. If the subscripts 1 and 2 refer to these isotopes and $(B)_1$ and $(B)_2$ are the second virial coefficients as determined experimentally, the quantum correction for isotope 1 is:

$$(B_q)_1=[(B)_1-(B)_2]/(1-M_1/M_2). \quad (27)$$

K. Schäfer[17] has measured the second virial coefficients for H_2 and for D_2 so that we can compare the calculated with the experimental quantum corrections in this case. Using the Lennard-Jones potential with the energy of repulsion varying inversely with the twelfth power of the separation, we calculate $(B_q)_{H_2}=0.0056$ at 45°A. From Eq. (27), $B_{H_2}-B_{D_2}$ is equal to $\frac{1}{2}(B_q)_{H_2}$ or 0.0028 whereas Schäfer finds this difference to be 0.0015. The agreement is as good as could be expected considering that the higher terms in Eq. (25) become important at low temperatures. As in the case of helium, these terms will make the quantum correction smaller than B_q. Schäfer has also calculated the quantum corrections for H_2 but unfortunately he attributed the total quantum correction to the discrete states with energy less than that of the separated molecules. Wigner[12] has shown that the quantum correction arising from the states of greater energy is equally important and, therefore we cannot regard the excellent agreement which Schäfer obtained as significant.

[17] K. Schäfer, Zeits. f. physik. Chemie **B36**, 85 (1937); **B38**, 187 (1937).

IV. The Form of the Assumed Potential Energy Function

The form which we assume for the potential energy function for use in the statistical mechanical formulae must be a compromise between accuracy and tractability. Lennard-Jones[18] has recently published a discussion of the various forms which are currently considered. At large separations both theory and experiment point to an energy of attraction varying as the inverse sixth power of the separation. Margenau[19] has shown that, at least in the case of hydrogen atoms and perhaps quite generally, an inverse eighth power attraction becomes important at slightly smaller separations. As the molecules approach they reach a point of minimum energy and repel each other on closer contact. It is only in the cases of interaction between two hydrogen,[20] two helium[21] atoms, and two neon atoms[22] that quantum-mechanical calculations for the repulsive energy are available. In these calculations as well as in the experimental studies of crystal lattice energies[23] it appears that the energy of repulsion decreases exponentially with the separation. In a study of van der Waals energy, however, we are only interested in the variation of this energy over a small range of separations, and therefore it will be permissible to approximate the exponential behavior by a repulsion energy varying as an inverse power. We therefore use the Lennard-Jones[24] potential

$$E(r)=-c/r^6+l/r^s. \quad (1)$$

With this function, Lennard-Jones has shown how to integrate the expression for the second virial coefficient, (18), in terms of a rapidly converging series. The use of an exponential repulsion in formula (18) is possible and has actually been used by Kirkwood and Keyes[25] for helium and by Herzfeld[26] for argon, but the work

[18] Lennard-Jones, Physica **4**, 941 (1937).
[19] H. Margenau, Phys. Rev. **38**, 747 (1931).
[20] Eisenschitz and London, Zeits. f. Physik **60**, 491 (1930); H. Eyring, J. Am. Chem. Soc. **54**, 3191 (1932).
[21] Slater and Kirkwood, Phys. Rev. **37**, 682 (1931); Slater, Phys. Rev. **32**, 349 (1928); Margenau, Phys. Rev. **38**, 747 (1931).
[22] Bleick and Mayer, J. Chem. Phys. **5**, 252 (1934).
[23] Born and Mayer, Zeits. f. Physik **75**, 1 (1932).
[24] Lennard-Jones, see for example Fowler's *Statistical Mechanics*, Chapter X and for his later work reference 18.
[25] Kirkwood and Keyes, Phys. Rev. **37**, 832 (1931).
[26] K. Herzfeld, Phys. Rev. **52**, 374 (1937).

entailed is sufficient to prevent its general application. The analysis which we make in this paper is directed at making subsequent analyses of the forces between molecules easy to perform. The Lennard-Jones potential is sufficiently flexible as to approximate the true potentials when the three constants c, l, and s are properly chosen, and yet it is easy to apply.

Substituting (1) into (19), Lennard-Jones obtained an expression equivalent to:

$$B=(2\pi N/3RT)r_0^3F_s(E_{\min}/kT) \qquad (28)$$

where $r_0=(l/c)^{1/(s-6)}$ is the internuclear separation for which $E(r)$ is zero, and

$$E_{\min}=-(1-6/s)c(6c/sl)^{6/(s-6)} \qquad (29)$$

is the minimum value for the potential energy of the two molecules with respect to the separated molecules as zero. The factor $2\pi Nr_0^3/3RT$ in Eq. (28) will be recognized as the second virial coefficient for rigid elastical molecules of collision diameter, r_0. F_s is then the correction factor to take into account the attraction between the molecules and the change of the collision diameter with temperature. Previous analyses[18] have shown that for many molecules s varies between 9 and 12, and the virial coefficients calculated with various values of s lie so close together that it is difficult to tell which value of s gives the best fit with experiment. The $F_s(E_{\min}/kT)$ are rapidly converging infinite series which must be tabulated for various values of s and of $E_{\min}/kT$. Fortunately, only a few values of s need be considered, and once these functions have been evaluated, they may be used in the analysis of many different substances. The function F_s of Eq. (28) has the explicit form:

$$F_s=y^{3/s-6}\left\{\Gamma\left(\frac{s-3}{s}\right)-\sum_{n-1}^{\infty}c_n(s)y^n\right\}, \qquad (30)$$

where

$$y=\left(-\frac{E_{\min}}{kT}\right)^{(s-6)/s}\frac{s}{6^{6/s}(s-6)^{(s-6)/s}}=\frac{c}{l^{6/s}(kT)^{(s-6)/s}} \qquad (31)$$

and

$$c_n(s)=3\Gamma\left(\frac{6n-3}{s}\right)\Big/sn! \qquad (32)$$

Lennard-Jones has published some of his curves for F_s but it is not possible to read them to the accuracy which is necessary in making an analysis. However, the values of F_s can be readily calculated using the values of $c_n(s)$ which are given in Table I.

Substituting the above expression for B into Eq. (11) and differentiating we obtain:

$$\mu_0=\frac{2\pi Nr_0^3}{3R}\left(\frac{R}{C_p{}^0}\right)G_s(E_{\min}/kT), \qquad (33)$$

where

$$G_s=y^{3/s-6}\left\{-\frac{3+s}{s}\Gamma\left(\frac{s-3}{s}\right)+\sum_{n=1}^{\infty}d_n(s)y^n\right\} \qquad (34)$$

and

$$d_n(s)=\frac{3}{s^2n!}[(3+s)+n(s-6)]\Gamma\left(\frac{6n-3}{s}\right). \qquad (35)$$

The values of $d_n(s)$ and of G_s are given in Tables I and II, respectively, while in Fig. 2, G_s is plotted against y. Since G_s is the correction factor of the Joule-Thomson coefficient to take into account the attractions between the molecules and the decrease in collision diameter as the collisions become harder, this figure shows us the qualitative trends in the change of the Joule-Thomson effect with temperature. We see plainly that at low temperatures μ_0 is positive; at a higher temperature it becomes negative and finally approaches zero. A similar study for F_s would show that $-B$ exhibits an analogous change with temperature.

In making the analysis with the Lennard-Jones potential, we fitted the experimental values of μ_0 at two temperatures, T_1 and T_2. From Eq. (33) it follows (if $C_p{}^0$ remains constant in this temperature range) that

$$(\mu_0)_{T_1}/(\mu_0)_{T_2}=G_s(E_{\min}/kT_1)/G_s(E_{\min}/kT_2). \qquad (36)$$

Different values of $E_{\min}$ were then tried to find the one which gives the value of the ratio agreeing with the experimental one. The value of G_s for this value of $E_{\min}/kT$ was then substituted into (33) to give r_0^3, the other constant characteristic of the molecular interaction. Fig. 2 is useful in deciding on a rough value of $E_{\min}$ to try as a first approximation.

TABLE I.

n	$c_n(9)$	$c_n(12)$	$c_n(15)$	$d_n(9)$	$d_n(12)$	$d_n(15)$
1	$8.9302 \cdot 10^{-1}$	$9.0640 \cdot 10^{-1}$	$9.1817 \cdot 10^{-1}$	1.488367	1.58620	1.65271
2	$1.66667 \cdot 10^{-1}$	$1.5318 \cdot 10^{-1}$	$1.4892 \cdot 10^{-1}$	$3.33333 \cdot 10^{-1}$	$3.44647 \cdot 10^{-1}$	$3.57408 \cdot 10^{-1}$
3	$5.0152 \cdot 10^{-2}$	$3.7766 \cdot 10^{-2}$	$3.3333 \cdot 10^{-2}$	$1.17022 \cdot 10^{-1}$	$1.03858 \cdot 10^{-1}$	$1.00000 \cdot 10^{-1}$
4	$1.65374 \cdot 10^{-2}$	$9.5735 \cdot 10^{-3}$	$7.3938 \cdot 10^{-3}$	$4.40996 \cdot 10^{-2}$	$3.11140 \cdot 10^{-2}$	$2.66178 \cdot 10^{-2}$
5	$5.55556 \cdot 10^{-3}$	$2.3604 \cdot 10^{-3}$	$1.5523 \cdot 10^{-3}$	$1.66667 \cdot 10^{-2}$	$8.85156 \cdot 10^{-3}$	$6.51966 \cdot 10^{-3}$
6	$1.85749 \cdot 10^{-3}$	$5.5845 \cdot 10^{-4}$	$3.0606 \cdot 10^{-4}$	$6.19163 \cdot 10^{-3}$	$2.37344 \cdot 10^{-3}$	$1.46907 \cdot 10^{-3}$
7	$6.1250 \cdot 10^{-4}$	$1.2645 \cdot 10^{-4}$	$5.6731 \cdot 10^{-5}$	$2.24582 \cdot 10^{-3}$	$6.00642 \cdot 10^{-4}$	$3.06350 \cdot 10^{-4}$
8	$1.98413 \cdot 10^{-4}$	$2.7424 \cdot 10^{-5}$	$9.9206 \cdot 10^{-6}$	$7.93651 \cdot 10^{-4}$	$1.43977 \cdot 10^{-4}$	$5.95238 \cdot 10^{-5}$
9	$6.3063 \cdot 10^{-5}$	$5.7079 \cdot 10^{-6}$	$1.6431 \cdot 10^{-6}$	$2.73273 \cdot 10^{-4}$	$3.28201 \cdot 10^{-5}$	$1.08443 \cdot 10^{-5}$
10	$1.96603 \cdot 10^{-5}$	$1.1427 \cdot 10^{-6}$	$2.5872 \cdot 10^{-7}$	$9.17482 \cdot 10^{-5}$	$7.14171 \cdot 10^{-6}$	$1.86276 \cdot 10^{-6}$
11	$6.0125 \cdot 10^{-6}$	$2.2053 \cdot 10^{-7}$	$3.8864 \cdot 10^{-8}$	$3.00625 \cdot 10^{-5}$	$1.4886 \cdot 10^{-6}$	$3.03141 \cdot 10^{-7}$
12	$1.80483 \cdot 10^{-6}$	$4.1119 \cdot 10^{-8}$	$5.5872 \cdot 10^{-9}$	$9.62576 \cdot 10^{-6}$	$2.9811 \cdot 10^{-7}$	$4.6932 \cdot 10^{-8}$
13	$5.3212 \cdot 10^{-7}$	$7.42 \cdot 10^{-9}$	$7.7083 \cdot 10^{-10}$	$3.01533 \cdot 10^{-6}$	$5.76 \cdot 10^{-8}$	$6.9375 \cdot 10^{-9}$
14	$1.54167 \cdot 10^{-7}$	$1.299 \cdot 10^{-9}$		$9.25002 \cdot 10^{-7}$	$1.072 \cdot 10^{-8}$	
15	$4.3927 \cdot 10^{-8}$	$2.2 \cdot 10^{-10}$		$2.78204 \cdot 10^{-7}$	$1.9 \cdot 10^{-9}$	

TABLE II.

$-E_{min}/kT$	y	G_9	$-E_{min}/kT$	y	G_{12}	$-E_{min}/kT$	y	G_{15}
0.006352	0.35	−0.43328	0.002500	0.10	−0.43310	0.002210	0.05	−0.48391
.009482	.40	− .45919	.008100	.18	− .52372	.007017	.10	− .57005
.013500	.45	− .47491	.010000	.20	− .53659	.022279	.20	− .61486
.018519	.50	− .47997	.015625	.25	− .55596	.043790	.30	− .57983
.032000	.60	− .45588	.022500	.30	− .55967	.10260	.50	− .37065
.050815	.70	− .38205	.040000	.40	− .52784	.1840	.7098	.00000
.062501	.75	− .32468	.050625	.45	− .49456	.22456	.80	.20287
.1175	.9256	.00000	.062500	.50	− .45062	.24358	.84	.30125
.14815	1.00	.20365	.075625	.55	− .39634	.27326	.90	.45865
.15264	1.01	.23439	.090000	.60	− .33206	.32572	1.00	.74804
.15722	1.02	.26594	.12250	.70	− .17371	.44141	1.20	1.43554
.25600	1.20	.99355	.14062	.75	− .07966	.57064	1.40	2.28705
.40652	1.40	2.24584	.1555	.7887	.00000	.71289	1.60	3.33463
.50001	1.50	3.10764	.16000	.80	.02446	.78874	1.70	3.94520
.52027	1.52	3.30334	.19360	.88	.21249	.86975	1.80	4.62245
.54107	1.54	3.50766	.20250	.90	.26369	1.03410	2.00	6.21054
.72786	1.70	5.50317	.25000	1.00	.54607			
			.30250	1.10	.87459			
			.36000	1.20	1.25327			
			.49000	1.40	2.18167			
			.64000	1.60	3.38508			
			.65610	1.62	3.52330			
			.7225	1.70	4.12008			
			.8100	1.80	4.94199			
			1.0000	2.00	6.96632			

Using (18) we can combine F_s and G_s to form η_0. Thus:

$$\eta_0=\frac{2\pi N r_0^3}{3R}\left(\frac{R}{C_v^0}\right)[F_s+G_s]$$

$$=\frac{2\pi N r_0^3}{3R}\left(\frac{R}{C_v^0}\right)H_s, \quad (37)$$

where $H_s=F_s+G_s$

$$=y^{3/s-6}\left[-\frac{3}{s}\Gamma\left(\frac{s-3}{s}\right)+\sum_{n=1}^{\infty}e_n(s)y^n\right] \quad (38)$$

and $$e_n(s)=\frac{3}{s^2 n!}\Gamma\left(\frac{6n-3}{s}\right)[3+n(s-6)]. \quad (39)$$

From these equations we see that at sufficiently high temperatures, i.e. small values of y, H_s and hence η_0 will become negative, in agreement with the observations of Roebuck and Osterberg. It is interesting to note that this was not the case in (24) when the collision diameter was assumed to be rigid.

V. The Equation of Corresponding States

It follows from Ursell's[8] development of the virial coefficients, that if $E(r)$ has the form

$$E(r)=E_0 f(r/r_0)$$

where E_0 and r_0 are constants characteristic of the molecule and $f(r/r_0)$ is a universal function for all substances, the theorem of corresponding states is valid. In the case of the Lennard-Jones form for the potential energy this would mean that s has the same value for many nonpolar substances. The equation of state can then be written in terms of reduced variables, P', V', T':

$$P'V'/T'=1+(P'/T')F_s(1/T')+\cdots, \quad (40)$$

where $P'=p/(E_{\min}/\frac{2}{3}\pi r_0^3)$, $V'=V/(\frac{2}{3}\pi N r_0^3)$,

$$T'=Tk/E_{\min}.$$

This equation has the important consequence that all of the properties of the substance which depend only on the equation of state will have the same values when expressed in these universal parameters. The virial, compressibility, and expansion coefficients are of this nature. From Eqs. (12) and (18) we see that $\mu_0 C_p^0$ and $\eta_0 C_v^0$ involve only the second virial coefficient and its derivatives and therefore have the same form for most nonpolar substances. The theorem of corresponding states is also useful in connection with the pressure dependent parts of the Joule-Thomson and free expansion coefficients which involve the specific heat C_v^0, a function of the internal configuration of the molecule, as well as the variables of state. Thus from Eq. (10) we see that:

$$\mu=r_0^3 f_1(P', T')/[(C_v^0/R)-f_2(P', T')], \quad (41)$$

where f_1 and f_2 are universal functions of the reduced pressure and temperature. To the approximation that $(C_v^0/R)=\frac{3}{2}$ for monatomic molecules, all of these substances would have a universal form for their Joule-Thomson coefficient; similarly diatomic molecules would fall into another class, etc. The relationship between these classes is given by (41). A knowledge of the functions f_1 and f_2 obtained from the experimental or theoretical study of Joule-Thomson coefficients for monatomic and diatomic gases should therefore be useful in predicting the Joule-Thomson coefficients for polyatomic molecules. Similarly from Eq. (16) it follows that:

$$\eta=r_0^3[(C_v^0/R)g_1(P', T') -g_2(P', T')]/[(C_v^0/R)+g_3(P', T')]. \quad (42)$$

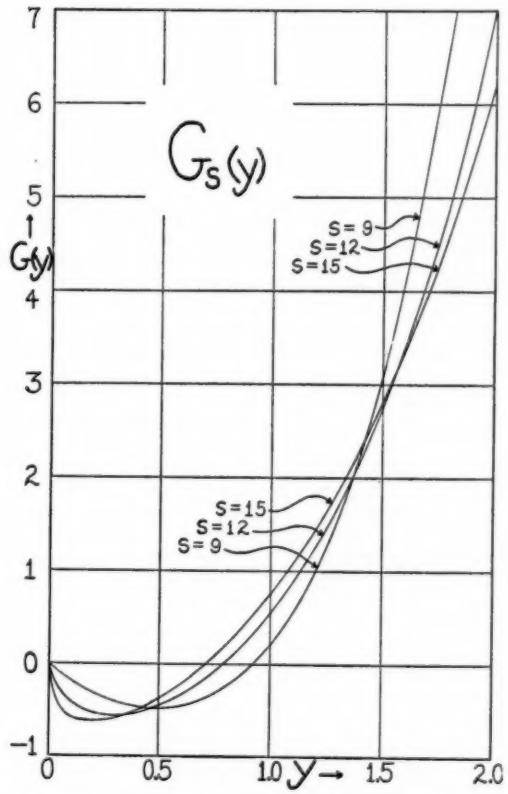

FIG. 2. G_s is plotted as a function of y. Since y is inversely proportional to the $(s-6)/s$ power of the temperature, small values of y correspond to high temperatures. The Joule-Thomson coefficient extrapolated to zero pressure is proportional to these G_s for all nonpolar substances to which the Lennard-Jones potentials apply.

The functions f and g occurring in (28) and (29) can be obtained explicitly from Eqs. (10) and (17) with the aid of (40).

One immediate application of the theorem of corresponding states is a connection between the temperatures for the Boyle point and for the (lower) Joule-Thomson inversion at low pressures. These points occur for different universal values of T'.

$$T_I/T_B=T'_I/T'_B, \quad (43)$$

where I and B refer to the inversion and Boyle points respectively. It follows that T_I/T_B should be very nearly the same for all nonpolar substances. Table III shows the values for this ratio which we obtained when the potential energy function was taken to be of the Lennard-Jones form with different values of s. Thus in the case of N_2 where the measurements of Roebuck and

Osterberg[27] give $T_I = 623^0$A, we would expect the Boyle point to lie between 333^0 and 329^0A. Actually the experimental determinations recorded in the *International Critical Tables* show that it is 325^0A which is satisfactory agreement.

VI. Analysis of the Joule-Thomson Data for Helium

Helium is one of the simplest gases to study. Its critical temperature is so low that at room temperature helium molecules behave almost like elastic billiard balls with little attraction between each other. Extensive theoretical and experimental studies of helium have been made. The only disagreeable feature of helium is the importance of the quantum-mechanical corrections which have to be made in its equation of state. Uhlenbeck and Beth inserted the Lennard-Jones potential into their equation and found that at 100^0A the quantum correction B_q is 11 percent of the classical second virial coefficient and that it is still 3 percent of B_{class} at 300^0A. Their numerical values for B_q can be expressed in the form: $B = B_{\text{class}} + B_q$ where

$$B_q = 1.13T^{-2} + 33T^{-3}. \tag{44}$$

Substituting this expression for the second virial coefficient into (12)

$$\mu_0 = (\mu_0)_{\text{class}} + (\mu_0)_q$$

where
$$(\mu_0)_q = -0.90T^{-1} - 40T^{-2}. \tag{45}$$

Here $(\mu_0)_q$ is the correction term to be added to the classical expression $(\mu_0)_{\text{class}}$ to obtain the experimental value μ_0. Comparing this correction term with the experimental results of Roebuck and Osterberg[28] we obtain Table IV. If this quantum correction is correct at least as to approximate magnitude, it becomes apparent that an analysis of the law of force between two helium molecules based on the classical statistical mechanical formulae would lead to an apparent potential energy quite different from reality. Wigner[12] has pointed out that the quantum-mechanical correction is extraordinarily sensitive to the exact form for the potential energy between the molecules. It is therefore difficult to estimate the accuracy of the Uhlenbeck and Beth quantum-mechanical correction and of the corresponding correction to the Joule-Thomson coefficient. We are particularly troubled by the discrepancy between the Uhlenbeck and Beth results and those of Kirkwood[29] who performed a similar analysis and obtained much smaller correction terms. Tentatively, we shall accept the Uhlenbeck and Beth results in our analysis, with the reservation that future work in this field may change the values of $(\mu_0)_q$ appreciably. We fitted the $(\mu_0)_{\text{class exp}}$ of Table IV with the aid of Eq. (39) and obtained a revised Lennard-Jones potential for helium which gives excellent agreement with the Roebuck and Osterberg determinations. The column marked $(\mu_0)_{\text{class calc}}$ was obtained with this function,

$$E(r) = -15.22\times10^{-61}/r^6 + 4.39\times10^{-106}/r^{12} \text{ ergs.} \tag{46}$$

This potential bears a striking resemblance to that of Slater and Kirkwood,

$$E(r) = -16.2\times10^{-61}/r^6 + 7.7\times10^{-10}\exp(-1.28r\times10^8) \text{ ergs,} \tag{47}$$

which was obtained from quantum-mechanical computations. Our potential gives $E_{\min} = -13.2\times10^{-16}$ ergs and $r_0 = 2.57$A whereas the Slater and Kirkwood function gives $E_{\min} = -14.4\times10^{-16}$ ergs and $r_0 = 2.58$A. Kirkwood and Keyes[25] have

Table III.

	Boyle Point		Inversion Point		T Inversion / T Boyle
s	$-E_{\min}/kT_B$	y_B	$-E_{\min}/kT_I$	y_I	
9	0.2195	1.1400	0.1175	0.9256	1.8683
12	.2924	1.0815	.1555	0.7887	1.8803
15	.3476	1.0398	.1840	0.7098	1.8895

Table IV.

$T^\circ A$	$(\mu_0)_{\text{exp}}$	$(\mu_0)_q$	$(\mu_0)_{\text{class exp}}$	$(\mu_0)_{\text{class calc}}$
80.9	−0.0365 deg. atm.$^{-1}$	−0.0172 deg. atm.$^{-1}$	−0.0193	−0.0200
88.9	− .0410	− .0152	− .0258	− .0257
116.8	− .0497	− .0106	− .0381	− .0384
172.1	− .0557	− .0066	− .0491	− .0498
273.1	− .0599	− .0038	− .0561	− .0568
297.5	− .0601	− .0034	− .0567	− .0574
374.2	− .0621	− .0027	− .0594	− .0590
472.6	− .0616	− .0021	− .0595	− .0595
575.5	− .0568	− .0017	− .0551	− .0585

[27] Roebuck and Osterberg, Phys. Rev. **48**, 450 (1935).
[28] Roebuck and Osterberg, Phys. Rev. **43**, 60 (1933).
[29] J. Kirkwood, Physik. Zeits. **33**, 39 (1932).

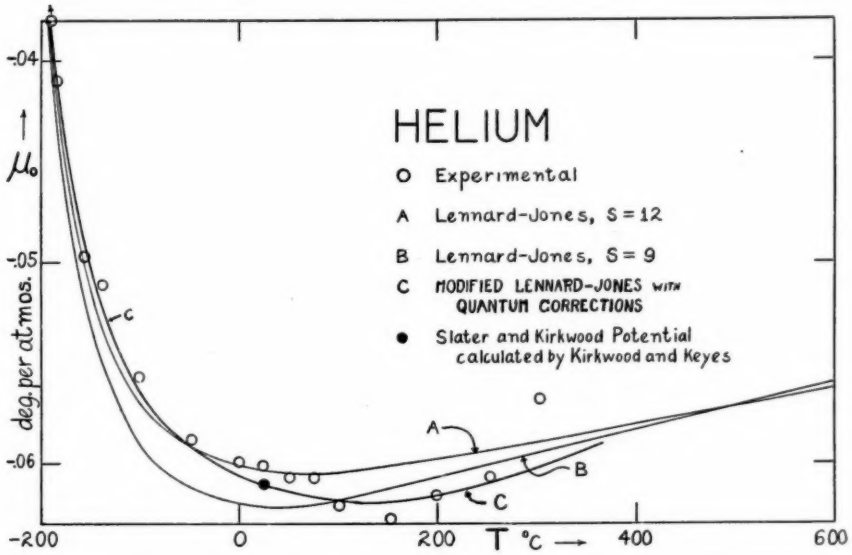

FIG. 3. The Joule-Thomson coefficient for helium is plotted as a function of temperature. The curves *A* and *B* were derived from the Lennard-Jones potentials in which the constants were adjusted so as to fit the experimental values of the second virial coefficient. The minimum in the Joule-Thomson coefficient indicates that the collision diameter of helium decreases with increasing temperature.

used the Slater and Kirkwood potential to compute the second virial coefficient. Their agreement with experiment is good, and this agreement would be further improved if the Uhlenbeck and Beth quantum corrections were used in place of those calculated by Kirkwood. Margenau[30] believes this to be fortuitous since he has shown that the induced dipole-quadrupole terms, which are neglected in the Slater-Kirkwood potential, are appreciable.

In Fig. 3 we have plotted:

1. The experimental Joule-Thomson coefficients of Roebuck and Osterberg.
2. The curves *A* and *B* obtained from the Lennard-Jones potentials with $s=9$ and $s=12$ from an analysis of the second virial coefficient neglecting quantum effects.
3. Curve *C*, our results using the modified Lennard-Jones function (μ_0 class calc) to which is added the quantum corrections $(\mu_0)_q$.

At the comparatively high temperatures in which we are interested, i.e., over 173°A, the effect of the attractive part of the potential curve is negligible, and for all practical purposes the helium molecules could be thought of as elastic billiard balls. Because the repulsive part of the potential curve is now the important one, the Joule-Thomson coefficient is negative, and the second virial coefficient is positive. But the collision diameter of the helium molecule decreases with the increased violence of the average collisions as the temperature is raised, and this gives rise to two rather interesting effects. The coefficient of free expansion becomes negative, and the Joule-Thomson coefficient passes through a minimum value. Neither of these effects could be caused in any other way. From the Slater and Kirkwood potential we see that the collision diameter, i.e., the value for r when $E(r)=\frac{1}{2}kT$, at room temperature is a half an angstrom smaller than at very low temperatures so that these qualitative arguments are sound.

Mayer and Harrison have recently computed the values of the third virial coefficient using the Lennard-Jones potential with $s=12$ and they have kindly made their results available to us in a private communication. Substituting their values for C into Eq. (12) it follows that $(\partial\mu/\partial p)^0_T=0.0005$. Of course, this computation is made neglecting the quantum corrections. Actually, to within the accuracy of their measurements, Roebuck and Osterberg did not observe any change of μ with pressure. It, therefore,

[30] Margenau, Phys. Rev. **38**, 1785 (1931); Proc. Nat. Acad. **18**, 56 (1932) and **18**, 230 (1932).

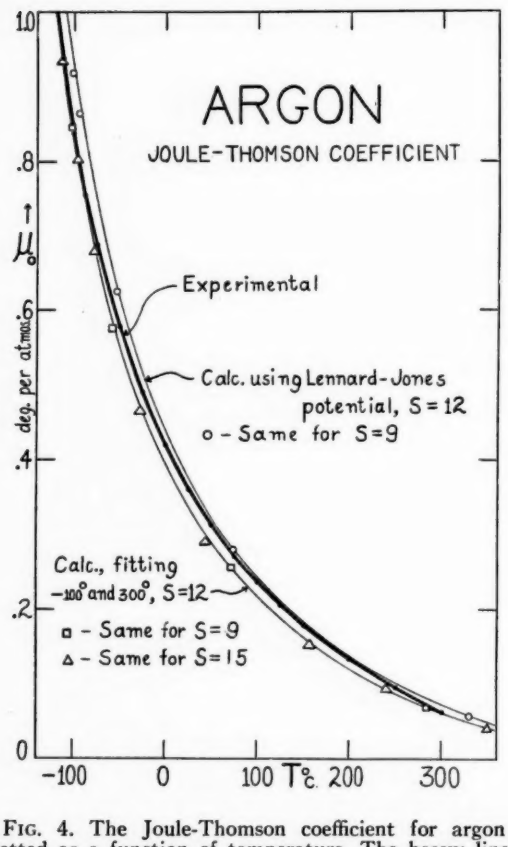

FIG. 4. The Joule-Thomson coefficient for argon is plotted as a function of temperature. The heavy line is from the experimental measurements of Roebuck and Osterberg. The line above the experimental curve is obtained from the Lennard-Jones potentials in which the constants were adjusted to fit the second virial coefficient data. The lower curve is an attempt to fit the Roebuck and Osterberg results by making the calculated and experimental results agree at −100°C and 300°C.

appears that the quantum correction is much more important in the case of third virials than it is for the second. Perhaps this might be expected since the third virial coefficient arises from three-body collisions. These collisions can be thought of as two-body collisions between double and single molecules. Since quantum considerations make these double species considerably less probable than would be expected on classical grounds, the third virial coefficient will be correspondingly smaller.

VI. Analysis of the Joule-Thomson Data for Argon

Argon, like helium, is a simple gas on which to test our methods of analysis. In some respects it is easier to study because the quantum corrections are negligibly small at ordinary laboratory temperatures. Unfortunately, the interactions between two argon molecules have not been studied theoretically, and our analysis must proceed purely inductively. Lennard-Jones has studied the second virial coefficients for argon and constructed potential functions which fit this data. But the absolute value of the second virial coefficient is difficult to measure accurately because it involves a knowledge of the volume of the gaseous system to many significant figures. Perhaps the inaccuracy of this constant is best illustrated by a direct comparison between the values of B for 0°C of Kammerlingh-Onnes[31] and of Holborn and Otto[32] which on conversion to our units are -7.3860×10^{-4} atmos.$^{-1}$ and -9.8509×10^{-4} atmos.$^{-1}$, i.e., a difference of 25 percent. The experimental measurement of the Joule-Thomson coefficient has the advantage that it provides a direct measurement of the imperfection of the gas in which this imperfection appears as a first rather than a second-order effect. Roebuck and Osterberg[33] have made some excellent measurements of the Joule-Thomson coefficient which we shall utilize. Their results for μ_0 are plotted in Fig. 4. An excellent empirical representation of their data is obtained by using the Herzfeld-Goeppert-Mayer potential where $r_0=3.43$A, $r_a=9.53$A and $D=2.37\times10^{-15}$ erg per molecule, the constants having been derived by fitting minus 100°, 100°, and 300°C. The Joule-Thomson coefficient calculated by Eq. (23) for this function agrees to within the experimental accuracy with the R. and O. data, but unfortunately we can attach little theoretical significance to it because the separation r_a at which the attractive potential ceases to be large is at a distance far in excess of any theoretical inter-

TABLE V.

T	$(\partial\mu/\partial p)^0_T$ calc.	$(\partial\mu/\partial p)^0_T$ obs.
573.2	−0.0007 deg/atmos.^{2}	−0.0002 deg/atmos.^{2}
473.2	− .0011	− .0005
373.2	− .0015	− .0009
273.2	− .0015	− .0012
173.2	− .0015	− .0030

[31] Kammerlingh Onnes and Crommelin, Leiden Communication **118b**, 24 (1910).
[32] Holborn and Otto, Zeits. f. Physik **33**, 1 (1925).
[33] Roebuck and Osterberg, Phys. Rev. **46**, 785 (1934).

action potential. The general characteristic that the potential should be shallow and that the attraction should extend over a large separation, may, however, have some significance. The Lennard-Jones curves, obtained by adjusting the constants in the potential energy function to fit the second virial data, agree with the experimental Joule-Thomson data at medium high temperatures but diverge at lower and higher temperatures. We changed these constants so as to fit the Joule-Thomson data at both 300°C and −100°C, but for no value of s, lying between 9 and 15 did the curves agree with R. and O. for the intermediate points. These curves are also shown in Fig. 4. It therefore appears that the experimental data is sufficiently accurate to warrant the use of a potential function more accurate than the Lennard-Jones type. Herzfeld[26] has recently computed the second virial coefficient for argon using the potential energy function which he and Goeppert-Mayer found to agree with crystal structure data. This function contains an exponential repulsion term instead of the inverse power, and it would be interesting to see how closely this potential would give results agreeing with Roebuck and Osterberg.

The quantum corrections are small in the case of argon. By substituting the Lennard-Jones potential with $s=12$ into Eq. (26) we find that at the lowest temperature that we are interested in, i.e., $T=173.2$A, B_q is only 2.54×10^{-5} which is less than one percent of the experimental second virial coefficient. This quantum correction would be even smaller by a factor of ten if argon molecules were rigid spheres with no attractions between the molecules. From the calculation at 173.2°A we estimate B_q by the form $B_q=0.76T^{-2}$. It follows that the quantum correction for μ_0 at 173.2°A is only $(\mu_0)_q=-0.0035$ or one-half of one percent of the experimental Joule-Thomson coefficient. Since this correction becomes smaller at higher temperatures it can be neglected. In Fig. 4, this quantum correction is roughly the width of the heavy black line.

The pressure dependence of the Joule-Thomson effect requires a knowledge of the higher virial coefficients as shown by Eqs. (10) to (14). Using Professor Joseph Mayer's and Miss Harrison's values for the third virial coefficients obtained from the Lennard-Jones potential with an inverse

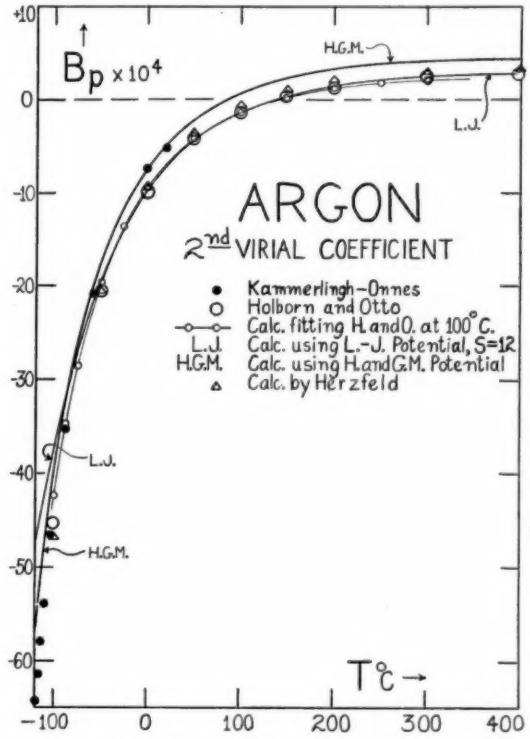

FIG. 5. The second virial coefficient of argon is plotted as a function of the temperature. The experimental points of Kammerlingh-Onnes and of Holborn and Otto are compared with the values calculated in different ways from the Joule-Thomson measurements of Roebuck and Osterberg. The values calculated by Herzfeld from a potential energy obtained from crystal structure data are also plotted.

twelfth power repulsion made, we obtained the values given in Table V of the change of the Joule-Thomson coefficient with pressure at zero pressure. The agreement between the calculated and the observed values is right as to the order of magnitude and the general trend, but the discrepancy is larger than we had anticipated. We have plotted in Fig. 5 the experimental second virial measurements of Kammerlingh-Onnes and of Holborn and Otto. Then we have drawn four curves. The first is a curve which we obtained by integrating the Joule-Thomson coefficients of R. and O. by Eq. (14) and evaluating the constant to fit H. and O's. second virial for $T=100$°C. The second is the curve obtained by the use of the Lennard-Jones potential with $s=12$. The third is that which we obtained from Eq. (32) using the Herzfeld-Goeppert-Mayer potential with constants derived from Joule-

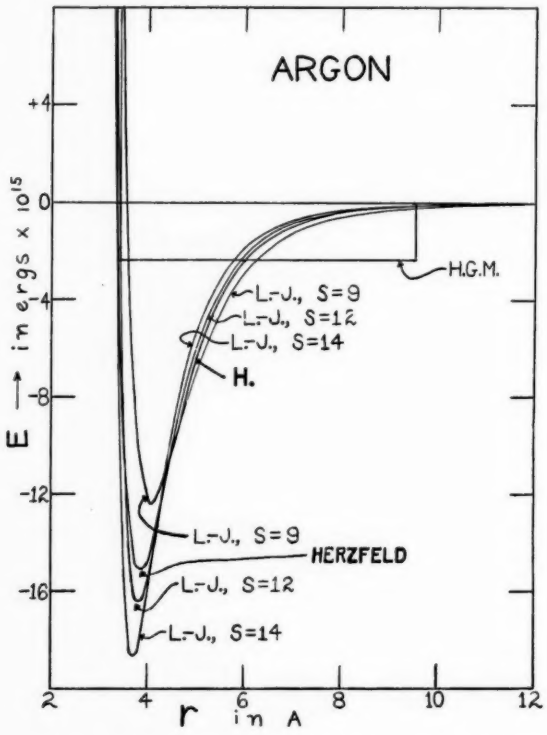

FIG. 6. The potential energy, E, of two colliding argon atoms is plotted as a function of their separation, r. The Lennard-Jones curves for $s=9$, 12, and 14 fit the experimental second virial and Joule-Thomson data equally well. The Herzfeld function is obtained from crystal structure observations. The Herzfeld and Goeppert-Mayer function which is quite different from any of these, still fits this data.

Thomson data. The fourth is that obtained by Herzfeld using his potential (with r in A):

$$E(r) = -1.11\times10^{-10}r^{-6} + 1.34\times10^{-9}\exp(-r/0.345) \text{ ergs.}$$

where the constants have been evaluated from a study of crystal structure. Of all of these functions, Herzfeld's seems to give the best agreement with experiment. The R. and O. curve, obtained by the integration and experimental evaluation of the integration constant, agrees nicely with all of H. and O.'s experimental data. The Lennard-Jones curve is satisfactory, compared with H. and O.'s data, at high temperatures, but deviates appreciably at the lower temperatures which is the same effect which we noticed in studying the Joule-Thomson effect. The H.G.M. potential results in agreement with Kammerlingh-Onnes.

In Fig. 6 we have plotted the potential energy function for argon. The Lennard-Jones curves all give about the same agreement with the Joule-Thomson data. The Herzfeld function is probably the most accurate. From the great difference between these functions we see the inherent uncertainty involved in the inductive method of determining the potential energy curves. The fact that the Herzfeld Goeppert-Mayer function also gives a good fit, makes this indeterminancy more apparent. The convergence of the inductive and of the theoretical approach should improve this situation. We should obtain from quantum mechanics at least some of the constants for the potential energy function as, for example, the van der Waals attractive potential, $-c/r^6$, and probably the Margenau inverse eighth power attraction term. Theoretical considerations should also determine the best form of the remainder of the potential and this will involve the only parameters to be determined from experiment.

We wish to thank Professor Eugen Wigner for helpful discussions, and express our gratitude to Professor Joseph Mayer and Miss Harrison for the use of their unpublished third virial coefficient computations. One of us (J.O.H.) would like to express his appreciation to the Wisconsin Alumni Foundation for financial support throughout the course of this work.

Note on the Free Energy of Acetylene

A. R. GORDON
Chemistry Department, University of Toronto, Toronto, Canada
(Received January 15, 1938)

ALTHOUGH acetylene is a reactant in a number of technically important gas reactions, moderately accurate free energy data are almost entirely lacking for it. Kassel[1] has computed F/T using the harmonic oscillator-rigid rotator approximation for its energy levels. Such an approximation, however, may introduce appreciable errors for high temperatures, and it is precisely the high temperature range that is of greatest experimental interest.

The most serious obstacle to a more exact calculation is the fact that attempts to represent the vibrational levels by an expression of the usual form

$$\epsilon_V = \sum_i v_i\omega_i + \sum_{ij} v_i v_j x_{ij} \qquad (1)$$

have met with only moderate success. As is well known, acetylene has seven vibrational degrees of freedom divided among five fundamental frequencies, designated in Herzberg's notation as: ν_1 a C—C frequency, ν_2 and ν_3 symmetrical and antisymmetrical C—H frequencies, ν_4 and ν_5 antisymmetrical and symmetrical doubly degenerate deformation frequencies. Recently Mecke and Ziegler[2] have attacked the problem from a new angle. They assume only three fundamentals: a C—C frequency ν_{CC}, a doubly degenerate C—H frequency ν_{CH}, and a quadruply degenerate deformation frequency δ. Through anharmonicity and electrical and mechanical coupling, the degeneracy is wholly or partly removed, and they give equations by which the separations of the resulting levels may be computed. For example, for $v_\delta=2$, there will be three energy states 1454, 1328 and 1218 cm^{-1} above the ground state, corresponding in the older notation to the levels ($v_4=2$, $v_5=0$), ($v_4=1$, $v_5=1$), ($v_4=0$, $v_5=2$). This theory has been adversely criticized by Childs and Jahn,[3] but the fact remains that it predicts energy levels in reasonably close agreement with those actually observed.

For the purposes of thermodynamic calculation, however, an expression of the type (1) is adequate provided the x_{ij} are average values determined from a large number of vibrational levels. The determinination of such averages is a matter of some difficulty, but for the present purpose those selected are: $\omega_1=1977.5$, $\omega_2=3392$, $\omega_3=3315$, $\omega_4=732.4$, $\omega_5=612.8$, $x_{11}=-4.5$, $x_{22}=-20$, $x_{33}=-32$, $x_{44}=-3.2$, $x_{55}=-1.0$, $x_{12}=x_{13}=-8$, $x_{23}=-100$, $x_{14}=x_{15}=0$, $x_{24}=x_{25}=x_{34}=x_{35}=x_{45}=-12.5$, all expressed in cm^{-1}. This choice is consistent with the most recent values of the fundamentals listed by Funke and Lindholm[4] *viz.* 1973, 3372, 3283, 729.2 and 611.8 cm^{-1}; for the energy states with $v_\delta=v_4+v_5\leqq 5$, $v_{CH}=v_2+v_3\leqq 5$, it introduces at most an error of 0.005 in F/T if it be assumed that the levels computed by Mecke and Ziegler's equations are the correct ones. Moreover, for some 40 levels listed by Funke and Lindholm, the use of this approximate expression instead of the experimentally observed values causes at most an error of 0.006 in F/T.

The rotational constants[4] are $B=1.1764-0.0051\,(v_{CH}+v_{CC})+0.0020v_\delta$; $D=-1.83\times10^{-6}$. For consistency with earlier free energy calculations, the universal constants are $R=1.9869$, $hc/k=1.4324$, additive constant for the translational free energy $=-7.267$. The resulting values[5] of $(F^0-E_0^0)/T$ for a few temperatures and of $S^0_{298.1}$ are given in Table I; in none of these entries is the nuclear spin contribution of the two hydrogen atoms in the molecule included. For purposes of interpolation, the entries can be represented within one or two units in the last decimal place as printed by the empirical equations below. These equations have been checked at numerous intermediate temperatures.

$$(400\text{–}1200^\circ\text{K})-(F^0-E_0^0)/T=0.223+16.0125\log T-18.3\log(1-\exp[-900/T])-1.068\times10^{-3}T+0.817\times10^{-6}T^2,$$

[1] Kassel, J. Am. Chem. Soc. **55**, 1351 (1933).
[2] Mecke and Ziegler, Zeits. f. Physik **101**, 405 (1936).
[3] Childs and Jahn, Zeits. f. Physik **104**, 804 (1937).
[4] Funke and Lindholm, Zeits. f. Physik **106**, 518 (1937).
[5] For the method of calculation, see Gordon, J. Chem. Phys. **3**, 259 (1935).

$$(1200\text{–}2800°\text{K}) - (F^0 - E_0^0)/T = -1.642 + 16.0125 \log T + 6.256 \times 10^{-3} T - 0.475 \times 10^{-6} T^2.$$

A comparison of the data of Table I with Kassel's values (after subtracting the nuclear spin contribution 2.754 cal./deg. from his numbers) shows that the values given here are slightly less than his for low temperatures, principally due to the fact that he used a slightly smaller value of ν_5, namely 600 cm^{-1}; for high temperatures, the values of Table I are definitely greater than his, owing primarily to the contribution of x_{45} to the state sum. For example, for 2000°, Kassel gives 61.59 cal./deg. (64.34 before subtracting the spin contribution) which is 0.24 cal./deg. less than the entry in Table I.

Kassel in his calculation adopts a heat of combustion for acetylene at 18°C of 311,000 cal.; from this and the known heats of combustion of hydrogen[6] and graphite[7] (68313 cal. and 94,240 cal. at 25°C) ΔH_{298} for the reaction $2C + H_2 = C_2H_2$ is 54150. From this and the thermodynamic data for hydrogen[8] and graphite[9] $\Delta F^0_{298.1}$ is 49970 cal. and ΔE_0^0 is 54280 cal. The resulting values for $\log K_1 = \log (P_{C_2H_2})/(P_{H_2})$ are given in the table. Fig. 1 gives a comparison

TABLE I. $K_1 = (P_{C_2H_2})/(P_{H_2})$; $K_2 = (P_{HCN})^2/(P_{C_2H_2})(P_{N_2})$.

T°K	$-(F^0 - E_0^0)/T$	$-\log K_1$	$-\log K_2$
298.1	39.993	36.64	5.18
300	40.044	36.39	5.14
400	42.477	26.53	3.71
600	46.368	16.69	2.29
800	49.499	11.78	1.59
1000	52.157	8.85	1.17
1200	54.49	6.90	0.90
1600	58.47	4.47	0.56
2000	61.83	3.01	0.37
2400	64.75	2.04	
2800	67.35	1.35	
$S^\circ_{298.1}$	48.029		

[6] Rossini, Nat. Bur. Stand. J. Research **6**, 1 (1931).
[7] Roth and Naeser, Zeits. f. Elektrochem. **31**, 461 (1925) as corrected by Clayton and Giauque, reference 9.
[8] Giauque, J. Am. Chem. Soc. **52**, 4816 (1930); Davis and Johnston, J. Am. Chem. Soc. **56**, 1045 (1934).
[9] Clayton and Giauque, J. Am. Chem. Soc. **54**, 2610 (1932).

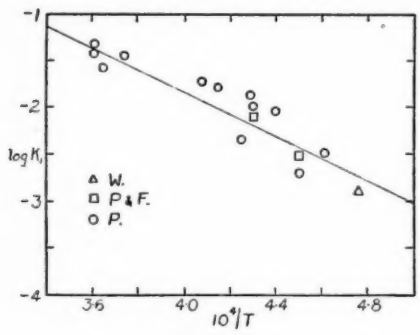

FIG. 1.

of the experimental values of $\log K_1$ obtained by Von Wartenburg,[10] by Pring[11] and by Pring and Fairlie[12] with the data of the table. The agreement is excellent, and is well within the limits of error of the experiments.

From the data for acetylene, nitrogen[13] and hydrogen cyanide[14] it is also possible to compute the equilibrium constant for the reaction $C_2H_2 + N_2 = 2\ HCN$. If the heat of formation of gaseous hydrogen cyanide at 298° be taken[14] as 31000 cal., ΔH_{298} for the reaction is 7850 cal.; $\Delta S^0_{298.1}$ is 2.659, hence $\Delta F^0_{298.1}$ is 7060 cal. Log $K_2 = \log (P_{HCN})^2/(P_{C_2H_2})(P_{N_2})$ is given in the last column of the table.

All the equilibrium constants of Table I are of course subject to correction as a result of the uncertainty in the heats of formation of acetylene and hydrogen cyanide. The former may be in error to the extent of 1 kcal. per mole, with a resulting uncertainty in $\log K_1$ of 0.09 at 2500°. The uncertainty for hydrogen cyanide must be considerably less than this, in view of the excellent agreement between the value computed for its free energy of formation from thermal and spectroscopic data, and that obtained from entirely independent equilibrium measurements.[14]

[10] Von Wartenburg, Zeits. f. anorg. allgem. Chemie **52**, 299 (1907).
[11] Pring, J. Chem. Soc. **89**, 1601 (1906); **97**, 498 (1910).
[12] Pring and Fairlie, Ind. Eng. Chem. **4**, 812 (1912).
[13] Giauque and Clayton, J. Am. Chem. Soc. **55**, 4875 (1933).
[14] Gordon, J. Chem. Phys. **5**, 30 (1937).

LETTERS TO THE EDITOR

This section will accept reports of new work, provided these are terse and contain few figures, and especially few halftone cuts. The Editorial Board will not hold itself responsible for opinions expressed by the correspondents. Contributions to this section must reach the office of the Managing Editor not later than the 15th of the month preceding that of the issue in which the letter is to appear. No proof will be sent to the authors. The usual publication charge ($3.00 per page) will not be made and no reprints will be furnished free.

The Near Infra-Red Absorption Spectrum of Sucrose Crystals in Polarized Light

A considerable amount of work has been done by different investigators upon the absorption of polarized infra-red waves in *inorganic* crystals. But little, if any, of this sort of work has been done with *organic* crystals. In the present study plane polarized waves in the region 0.8–2.5μ were sent through two specimens of sucrose crystals, 2.26 and 0.92 mm thick, respectively. Sucrose belongs to the hemimorphic hemihedral class of the monoclinic system having three axes of unequal lengths, one perpendicular to the plane of the other two. The b axis, a twofold axis of symmetry, is perpendicular to the plane made by the a and c axes which make an angle β of 103° 30′ with each other. The crystals were placed one at a time directly before and in contact with the slit of the recording spectrograph, with the b axis vertical and the c axis horizontal and with the rays traveling approximately along the a axis. Polarization was accomplished by using a Glan-Thompson prism. Because this prism transmits the extraordinary ray only, the absorption bands produced by the calcite of the prism are not strong in spite of the 5 cm length of the prism. Records were obtained with each specimen with the light polarized parallel to the b and the c axes. Complications arising from optical rotation are negligible. The following features of interest were revealed.

(a) Relatively sharp bands at 1.44μ and 0.98μ, regarded as first and second overtones, indicate that unperturbed OH groups exist in the crystal lattice. These bands have greater intensities when the electric vector of the wave oscillates along the b axis than when along the c axis. Assuming that the electric moment with which the light vector interacts is localized in the OH group and that the magnitude of the interaction depends upon the square of this moment, and taking into account the logarithmic law of absorption, one can estimate that there is a 50 percent greater alignment of unperturbed OH groups along the b axis than along the c axis.

(b) A broad doublet band with components of nearly equal intensities at 1.51μ and 1.58μ is regarded as the perturbed counterpart of the 1.44μ band. The 1.51μ and 1.58μ bands, separated respectively from the 1.44μ band by wave number intervals $\delta = 320$ cm^{-1} and $\Delta = 620$ cm^{-1}, are regarded as arising from OH oscillators perturbed through hydrogen bridges, the H of the bridge belonging to the OH oscillator in the latter instance and to another OH group in the former instance. This interpretation arises from the perturbation concepts put forth by Cross, Burnham and Leighton[1] in connection with their interpretation of the Raman spectrum of water. These authors regard the water vapor molecule as two coupled OH oscillators, and regard liquid water molecules as coupled OH oscillators perturbed in the δ and Δ manners indicated above. It is interesting to note that the ratio $\Delta : \delta$ has approximately the 2 : 1 value assumed by Cross, Burnham and Leighton. The larger magnitudes of the perturbations found here are believed to arise, not because of any great difference in the nature of the H bridge, but rather because of the greater amplitudes involved in the *overtone* vibrations than in *fundamental* vibrations. This remark is based upon a comparison of the widths of fundamental and overtone absorption bands of water, and also upon a pronounced difference in the fundamental[2] and overtone[3] regions of the wave number separations between the bands characteristic of associated and unassociated alcohol molecules.

The 1.51μ component of the sucrose spectrum shows greater absorption when the light vector vibrates along the b axis, but the 1.58μ one remains about the same for both types of polarization. This difference in behavior indicates separate origins for the two broad components, an interpretation which is consistent with the explanation given above.

There is a striking similarity between the bands of (a) and (b) and the bands in the spectra of the alcohols,[3] and a corresponding perturbation explanation seems possible with liquid alcohols.

(c) The 1.7μ absorption band associated with CH groups in gaseous and liquid molecules also appears in these spectra of sucrose crystals. It has, in this instance, four main components and the ratios of intensities among the components alter with a change in the plane of polarization.

The spectroscopic evidence for the existence of both free and perturbed OH groups is in good agreement with the model for the arrangement of the sucrose molecules in the unit cell as suggested by x-ray crystal analysis.[4] The sucrose crystal has been found to have two molecules per unit cell, the dimensions of which are $a_0 = 11.06$A, $b_0 = 8.84$A and $c_0 = 7.76$A and $\beta = 103° 30'$. On the basis of the asymmetry of the molecule, the number of molecules in the unit cell and the halving of the 0 1 0 plane, sucrose is placed in the space group C_2^2, in which case there should be a molecule of sucrose located at one point in the lattice and another rotated through 180° at half the unit distance

from this along the b axis. Chemical evidence indicates that the most probable structure for sucrose is α-glucopyranose-β-fructofuranose. Using the three criteria of cell dimensions, space group symmetry and cleavage planes this molecule is found to fit into the unit cell best with its long axis parallel to the short diagonal of the unit cell, i.e., the $\bar{1}\,0\,1$, and the flat sides of the rings parallel to the $0\,1\,0$. In such an arrangement the hydroxyl groups between the flat rings of adjacent molecules along the b axis approach to within 2.5–3A of each other. This at once suggests the existence of hydrogen bridges along the b axis between adjacent molecules, a view which is substantiated by the fact that cleavage planes parallel to the $0\,1\,0$ do not occur. On this basis it is possible to compute that there are in the unit cell probably about four free OH groups and twelve OH groups perturbed by hydrogen bridges, six each in the Δ and δ manners. It is believed that, owing to spatial restrictions within the crystal lattice, only these two types of perturbation occur. Since the hydrogen bridging is assumed to be associated only with OH groups, the numbers perturbed in Δ and δ fashions must be equal. This equality is consistent with the approximate equality in the intensities of absorption in the 1.51μ and 1.58μ bands.

The results of this study indicate that infra-red absorption spectroscopy involving polarized light may be a useful adjunct to x-ray analysis of organic crystal structures. For, the most intense absorption bands, at least in the *near* infra-red, are associated with hydrogen atoms, which are just the ones whose locations x-ray analysis is unable to determine. Of course, infra-red analysis cannot locate single atoms in crystals, but the dependence of intensity of absorption upon plane of polarization should be able to give the relative number of alignments in different directions of specific groups, such as OH groups.

JOSEPH W. ELLIS
JEAN BATH

University of California,
Los Angeles, California,
March 14, 1938.

[1] Cross, Burnham and Leighton, J. Am. Chem. Soc. **59**, 1134 (1937).
[2] Errera and Mollet, Nature **138**, 882 (1936).
[3] Kinsey and Ellis, J. Chem. Phys. **5**, 399 (1937).
[4] Unpublished work of J. D. Bath and O. L. Sponsler, University of California at Los Angeles.

The Liquid State

In the description of the liquid state which they are developing, Eyring and Hirschfelder[1] more than once stress the fact that in their theory the *total* free volume in a liquid, as in a gas, is shared by all the molecules; in the entropy of melting of a simple substance the most important term is the contribution R, arising from the fact that the entire free volume is jointly used by all the molecules.

It will be suggested below that we can perhaps obtain a clearer idea of the difference between the liquid and solid states, if we recognize that almost the whole of the additional entropy of a simple liquid arises from the local relationship between a molecule and its neighbors. About

FIG. 1.

nine-tenths of the communal entropy R is due to a purely local sharing of free volume between a molecule and its immediate neighbors—a sharing of free volume which is intimately connected with those small fluctuations, which are impossible in a solid, but which in a liquid permit the viscous flow.

Consider first one mole of a gas contained in a fixed volume in which the partition function of a single molecule is f. Now suppose that by means of numerous partition walls the entire volume is divided into cells of equal size, each containing the same small number n of molecules (less than ten). The partition function for a molecule in any cell is now fn/N, and there are N/n cells. The entropy of the whole gas is

$$(N/n)(n \log (fn/N) - \log n!)k.$$

When there is one particle per cell ($n=1$), the gas, as Hirschfelder and Eyring[2] have pointed out, is comparable with a solid, its entropy being $Nk \log f/N$. If, starting with $n=1$, we remove a few of the dividing walls, until in each cell n becomes equal to, say, 5, the increase in entropy is given by

$$\Delta S = R\left(\log\frac{fn}{N} - \frac{1}{n}\log n!\right) - R\log\frac{f}{N} = R\left(\log n - \frac{1}{n}\log n!\right).$$

For $n=5$ this already has the value $0.655R$, and Fig. 1 shows how rapidly the value of ΔS rises with increasing n. If the gas is degenerate, $n!$ in the above expressions must be replaced by a number smaller than $n!$, which makes the entropy increase still more rapidly.

These ideas are applicable to a liquid, if in place of the volume we introduce the free volume of the molecules. Inside any one cell the molecules will share their free volume in common. It appears that when each cell contains only 27 molecules the entropy of the liquid already amounts to 90 percent of its value for a liquid with unconstrained molecules.

R. W. GURNEY
N. F. MOTT

University of Bristol,
Bristol, England,
March 4, 1938.

[1] Eyring and Hirschfelder, J. Phys. Chem. **41**, 249 (1937). Kincaid and Eyring, J. Chem. Phys. **5**, 587 (1937).
[2] Hirschfelder, Stevenson and Eyring, J. Chem. Phys. **5**, 896 (1937).

The Secular Equation for Molecular Vibrations

It is well known that when the potential and kinetic energies of a vibrating N atomic molecule are expressed in terms of the $3N$ Cartesian coordinates of the atoms, the secular equation for the vibration frequencies has $3N$ rows and columns and $3N$ roots, six of which are equal to zero. Recently, Redlich and Tompa[1] have published a method for manipulating such a secular equation so as to eliminate the zero roots and obtain a new equation of only $3N-6$ rows and columns. It is the purpose of this letter to give a much simpler method which accomplishes essentially the same results as theirs and to outline the drawbacks of both these methods as contrasted with a number of others which have been previously described.

By direct elimination of p_2 between Eq. (13) and (14) of Redlich and Tompa's paper, one obtains

$$\{B_{11}-B_{12}M_{22}^{-1}F_{22}^{-1}F_{21}M_{11}-\omega^2 M_{11}\}p_1=0,$$

in which their notation has been employed. If the F matrix is adjusted so that $F_{22}=E$, as they recommend, the secular equation becomes

$$|B_{fu}-\sum_u B_{fu}F_{ug}M_g/Mu-\omega^2 M_g\delta_{fg}|=0.$$

This equation requires all the potential constants B_{ij} but involves only one summation, whereas Redlich and Tompa's equation requires somewhat fewer constants but two summations.

Unfortunately, both these methods suffer from the very grave defect of yielding an unsymmetrical secular equation. The two easiest methods of solution of large secular equations, the method of numerical approximation[2] and the mechanical method,[3] both require an equation symmetrical with respect to the principle diagonal. The numerical method can be modified to remove this limitation, but it then becomes very considerably more laborious. Since this is true, and since any manipulation which yields a symmetrical secular equation is equivalent to a change of coordinates,[4] we believe that the older methods of eliminating the zero roots are still to be preferred.

The problem of the elimination of zero roots is independent of the question of the factoring of the secular equation by the use of the symmetry of the molecule. In symmetrical molecules, $3N$ linear combinations of the Cartesian coordinates can be constructed, not involving the relative masses of the atoms, which have the proper symmetries to factor the secular equation. These *external symmetry coordinates*, which Redlich and Tompa denote by p, can be used instead of the Cartesian coordinates with the result that the discussions of this letter then apply to each factor instead of to the whole secular equation. The number of zero roots in a given factor may be less than six.

If the number of rows of a given factor of the secular equation is small, say three, it is simplest to expand the determinantal equation into an ordinary algebraic equation, from which the zero roots can be eliminated immediately. For larger factors there are several possible procedures. One is to leave the secular equation unaltered and solve by numerical or mechanical methods. This has the drawback of requiring the solution of a larger secular equation than would be required if the zero roots were removed, but has the advantage that the secular equation is quickly and easily set up.

Another method is to employ *internal* coordinates ($3N-6$ in number) such as interatomic distances and angles. This gives a secular equation with no zero roots and $3N-6$ rows and columns. ("Geometrical symmetry coordinates"[5] are of this type and in addition utilize the symmetry to factor the equation.) The drawbacks of this type are, first, the difficulty of obtaining the kinetic energy expression, and second, the fact that the kinetic energy contains cross terms, so that the numerical solution is more difficult and the mechanical method inapplicable.

Still another procedure is to eliminate six of the Cartesian coordinates from the kinetic and potential energy expressions by means of the conditions of the linear and angular momenta. This gives a symmetrical secular equation but the kinetic energy again contains cross terms, and in addition the whole process is rather cumbersome.

Finally, a set of coordinates[6] may be used with the following properties: (a) Six of them represent the motions of translation and rotation. (b) In terms of these coordinates the kinetic energy matrix is the unit matrix. Such a set of coordinates produces a secular equation which is symmetrical, has no cross terms in the kinetic energy, and has the zero roots factored out. It is therefore in the form best suited for either numerical or mechanical solution. However, it is sometimes fairly troublesome to obtain these coordinates.

In conclusion, it is our experience that for small factors (less than four rows) it is best to expand the secular equation, which is originally set up in terms of external symmetry coordinates and therefore may contain zero roots. For larger factors, it seems best either to leave the zero roots in the equation and suffer the consequent larger sizes of the factors, or to transform to the type of symmetry coordinates which conserve momenta and therefore reduce the sizes of the factors.

E. Bright Wilson, Jr.
Bryce L. Crawford, Jr.*

Department of Chemistry,
Harvard University,
Cambridge, Massachusetts,
February 18, 1938.

* National Research Fellow in Chemistry.

[1] O. Redlich and H. Tompa, J. Chem. Phys. **5**, 529 (1937).
[2] H. M. James and A. S. Coolidge, J. Chem. Phys. **1**, 834 (1933); B. L. Crawford, Jr. and P. C. Cross, J. Chem. Phys. **5**, 624 (1937).
[3] D. P. MacDougall and E. B. Wilson, Jr. J. Chem. Phys. **5**, 940 (1937).
[4] M. Bocher, *Introduction to Higher Algebra*, p. 299 ff.
[5] J. E. Rosenthal and G. M. Murphy, Rev. Mod. Phys. **8**, 317 (1936).
[6] If it is required in addition that these coordinates have the proper symmetry properties to factor the secular equation, they become the "symmetry coordinates" of Howard and Wilson, (J. Chem. Phys. **2**, 630 (1934)). These coordinates have been criticized as unsuitable for use in connection with the isotope effect because they involve the atomic masses. We cannot understand this criticism because the secular equation will always contain the atomic masses in any event, and to change from one isotopic molecule to another of the same symmetry requires the same operations no matter what coordinates are used, whereas if the introduction of the isotopic atom lowers the symmetry, a new secular equation is necessary anyway. We have found these coordinates very useful.

The Polarization of the Absorption Lines of Single Crystals of Rare Earth Salts

The absorption spectra of rare earth salts of the type $M_2(SO_4)_3 \cdot 8H_2O$ have been studied in great detail, at different temperatures, by Spedding and his collaborators.[1] From a preliminary analysis of these spectra they have concluded that the electric fields acting on the rare earth ions in these crystals, which are responsible for the splitting of the energy levels of the ions, should be nearly cubic in symmetry. Since the absorption spectra of these crystals are complicated and their analysis difficult, it would be desirable to verify this conclusion by an independent method. One direct result of such a cubic symmetry for the electric fields is that the crystals should be magnetically isotropic. But actually many of these crystals are strongly anisotropic,[2] showing that the fields should deviate considerably from cubic symmetry.

The purpose of the present note is to show that some of the features of the absorption spectra themselves point to such a deviation from cubic symmetry in the internal electric fields. From a study of the absorption spectra of single crystals of these salts in polarized light, it is found that many of the absorption lines are strongly polarized, some of them being confined almost wholly to vibrations along one or another of the principal axes of the optical ellipsoid of the crystal, and that these variations in the direction of polarization occur even among the lines of the same group; in other words, among the Stark components

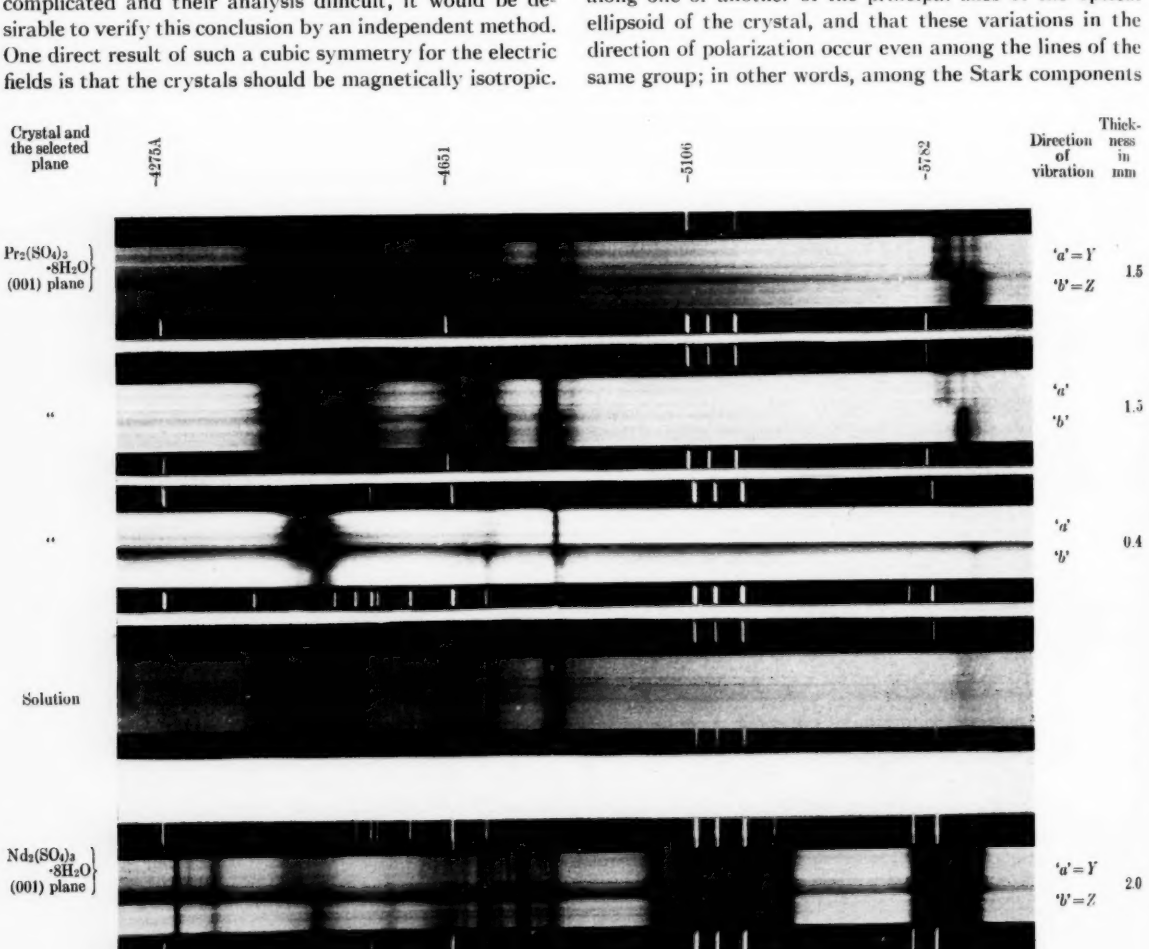

FIG. 1.

which originate from the same absorption line of the free ion, some are polarized strongly in one direction and some strongly in another.

We reproduce in Fig. 1 some typical absorption photographs which show the polarization. The crystals are monoclinic, and the upper and the lower halves in each photograph correspond to light vibrating respectively along the two extinction lines in the particular crystal plane selected for study.

The strong polarization, and the variation in its direction, observed among the members of a Stark group, show that the electric fields which produce the Stark splitting should be strongly asymmetric. Since there are 8 rare earth ions in the unit cell of the crystal, and the principal axes of the electric fields acting on these 8 ions may not be all parallel, the noncubic parts of the fields may be even much larger than the observed polarizations would suggest.

We are studying the polarization of the lines in some detail in the hope that the results may be helpful in the analysis of these complicated spectra.

K. S. KRISHNAN
D. C. CHAKRABARTY

Indian Association for the Cultivation of Science,
210 Bowbazar Street,
Calcutta, India,
January, 24, 1938.

[1] Several papers in this journal, 1937.
[2] K. S. Krishnan and A. Mookherji, Nature **140**, 549 (1937), and paper in course of publication in Phil. Trans. Roy. Soc. A.

The Infra-Red Absorption Spectrum of Nickel, Carbonyl Vapor

We have examined the infra-red absorption spectrum of nickel carbonyl between 1 and 20μ. The bands observed are shown in Table I, and compared with the Raman spectrum as observed by Duncan and Murray.[1]

The figures in parentheses indicate two complex and extended regions of absorption near 7.5 and 10μ; the former appears to have six or seven peaks at intervals of approximately 20 cm^{-1}.

The question at once arises as to whether free CO was present. The fundamental band of this substance as determined with a fluorite prism[2] has its center at 2146, with P and R branches easily resolvable at a separation of some 46 cm^{-1}: the Raman line[3] lies at 2155 10 cm^{-1}. A weak frequency in the $Ni(CO)_4$ infra-red spectrum shows as a side maximum at 2134 on the 2051 band. We found no trace of structure in the side band but cannot definitely say that it is not due to carbon monoxide. We propose to examine the effect of additions of small quantities of the gas on the spectrum in this region.

Evidence from electron diffraction measurements favors a tetrahedral model;[4] in this case the numbers of frequencies and their spectral characteristics are:

A_1: Two; Raman active, polarized;
E: Two; doubly degenerate, Raman active, depolarized;
F_1: One; triply degenerate, inactive in both Raman and IR;
F_2: Four; triply degenerate, active in both Raman and IR, depolarized.

TABLE I. *The Raman and infra-red spectrum of* $Ni(CO)_4$.

Raman	Intensity	100	20	8		4	
	Polarization	P	p	D			
	Frequency	82	382	463	—	601	—
IR	Frequency	—	—	—	542	—	655, 669, 684
	Intensity				m		w
Raman	Intensity	0			2	2	2
	Polarization						
	Frequency	718	—	—	833	872	913
IR	Frequency	—	757	787	826, 842	—	917
	Intensity		s	m	m		m
Raman	Intensity					0	
	Polarization						
	Frequency	—	—	—		1609	—
IR	Frequency		(983)	(1340)	1589	—	1677
	Intensity		m	m	m		w
Raman	Intensity		30	5	1		
	Polarization		p				
	Frequency		2043	2132	2223	—	—
IR	Frequency		2051	2134	—	2326	2476
	Intensity		$v.s.$	w		m	s

The coincidence of the high frequencies at 2043 and 2051 cm^{-1} would make it necessary to attribute these to the out-of-phase CO motions in F_2; the in-phase motion might then be 2223 cm^{-1} but this line should be powerful in the Raman effect and highly polarized. Further inspection of the data will show that other difficulties exist.

The plane square model was discussed by Bright Wilson[5] who showed that there should be 7 active Raman lines and 6 infra-red with no coincidences. Although those observed lie in the shorter wave region of the spectrum where one might anticipate their chance occurrence in combination tones due to many fundamentals, on the whole the evidence seems to support the tetrahedral model.

An approximate estimate of the Ni–C and C–O bond force constants gives 2.35 and 17.35$\times 10^5$ dynes/cm.

C. R. BAILEY
ROY R. GORDON

The Sir William Ramsay and Ralph Forster Laboratories,
University College, London, England,
February 15, 1938.

[1] J. Chem. Phys. **2**, 636 (1934).
[2] E. von Bahr, Verhand. Deutsch. Physikal. Gesell. **15**, 710 (1913).
[3] F. Rasetti, Proc. Nat. Acad. Sci. **15**, 234 (1929).
[4] L. O. Brockway and P. C. Cross, J. Chem. Phys. **3**, 828 (1935).
[5] J. Chem. Phys. **3**, 59 (1935).

Low and High Raman Frequencies for Water

I have read with some delay the remarks of I. Ramakrishna Rao and P. Koteswaran published by this journal[1] on "Low and High Raman Frequencies for Water." These authors state that of the Raman bands of water: 172, 510, 780, 1645, 2150, 3990 cm^{-1}, observed since 1933 by different workers using as exciting line the 2537A of the mercury arc, only the band 1645 cm^{-1} is genuine.[2] The authors consider all other bands as excited by lines of the mercury arc excepting 2537A, with an average shift of 3400 cm^{-1}, corresponding nearly to the center of gravity of the well-known very intense group of frequencies 3200, 3435, 3620 cm^{-1}.

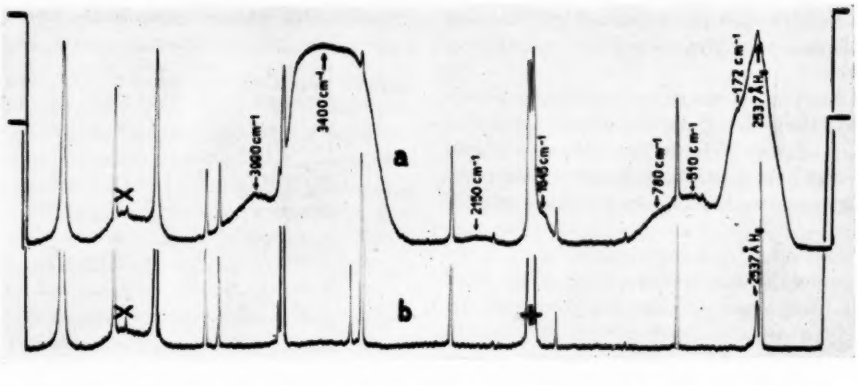

FIG. 1. The Raman bands of water (curve *a*) fall off (curve *b*) when the resonance line 2537A of the employed low pressure mercury arc is absorbed.

Without any doubt, this statement is to be attributed, as indicated by J. H. Hibben,[3] to the great differences between the mercury lamps at low pressure, exclusively used by the former workers, and the ordinary lamps, apparently used by Rao and Koteswaran. In the first type of lamps the resonance line 2537A is remarkably sharp and particularly intense (a thousand times more than any neighboring line); in the other type of lamps the same line, instead, is greatly weakened by self-reversal, so that it does not at all assume a prominent position between the other lines.

For that reason, and because the lines accompanying the 2537A are too numerous, and some are diffused, the ordinary lamps are absolutely unallowable in Raman work in ultraviolet. With their use to study the Raman spectrum of water, one cannot do better than observe the very intense group of frequencies at 3400 cm^{-1} excited by the various lines, and so do Rao and Koteswaran. The weak frequencies 172, 510, 780, 1645, 2150, 3990 cm^{-1} indeed, either are not photographed or, if photographed, are masked by the numerous bands corresponding to the quoted intense group of frequencies.

Independently of these considerations, it is to be noted that in 1933, when I have observed the frequencies in question, I have carried out and published an experiment to decide definitely its assignment.[4] In my experiment, a filter of mercury vapor at about 200°C was used in order to absorb, in the exciting spectrum of the low pressure mercury arc, the resonance line 2537A. I am giving in Fig. 1 two microphotometric curves of a plate made in 1933: *a* is the complete Raman spectrum of water obtained *without* the mercury filter, *b* is obtained *with* the mercury filter (3*h*, 30*m* and 3*h* exposures, respectively). I feel that no doubt will remain that the frequencies 172, 510, 780, 1645, 2150, 3990 cm^{-1} *really exist:* it is a fact that they fall off when the line 2537A is absent in the exciting spectrum.

The band indicated with a cross in both the curves has been considered by M. Magat[5] corresponding to a frequency 5100 cm^{-1}, as excited by the line 2537A. It is evident that it should be considered as excited by the group of lines at 2653A (indicated with plus sign in *b*), with the resulting displacement of about 3400 cm^{-1}.

G. BOLLA

Istituto di Fisica della R. Università,
Milano, Italy,
March 4, 1938.

[1] I. Ramakrishna Rao and P. Koteswaran, J. Chem. Phys. **5**, 667 (1937).
[2] There are some discrepancies, generally not essential, between the values given by different authors. I am referring the values given by me in Nuovo Cimento **10**, 101 (1933); in this paper I have also measured the low frequency 60 cm^{-1}, not afterwards observed by other authors. On this frequency and on the pointed discrepancies I will return elsewhere.
[3] J. H. Hibben, J. Chem. Phys. **5**, 994 (1937).
[4] G. Bolla, Nuovo Cimento **10**, 101 (1933), §3.
[5] M. Magat, J. de phys. **5**, 347 (1934).

Viscosity of Monomolecular Films

There have appeared in the numbers of *Nature* of September 11, 1937 and of the *Journal of Chemical Physics* of January, 1938, two editorial letters by Harkins and Myers, and Harkins and Kirkwood, respectively, concerning a surface viscosimeter. We wish to call attention to the previous results that we have obtained with a viscosimeter of the same type.[1]

We have shown experimentally that the surface flow per second, Q, is in fact proportional to the difference of pressure and inversely proportional to the length of the canal, but we think it necessary to insist that there is no law analogous to Poiseuille's law concerning the width of the slit. The corresponding Poiseuille equation for a two-dimensional fluid should contain a factor d^3 (d = width of slit). The results of our systematic study with canals of different widths show clearly that the problem is much more complicated. There is no doubt that we have simultaneous entrainment of the water and that the viscosity of the substrate becomes the preponderant factor as soon as canal widths of the order of one centimeter are reached, i.e. the flows per unit time become independent of the nature of the fluid as the diameter increases, finally reaching the same value. The relation with d^3 would be valid only as a limiting law for very narrow canals, since, as the diameter decreases, we find *linear* variation until

5 mm, this variation gradually changing to d^2 at 0.5 mm.

We think that even with corrective terms one can hope to attain only the order of magnitude of the two-dimensional viscosity of the film. The calculation made by Kirkwood is valid only for a deep canal, which is not the case for the viscosimeters used by us and by Harkins. The theory introduced by Bresler and Talmud[2] would give results in better qualitative accord even for large canals, although it introduces arbitrarily a frictional term proportional to the speed in the differential equation. Unfortunately, an error in the integration prevented these authors from observing the accordance cited above.

The correct integrated form should be:

$$Q=\frac{2\phi}{SA\kappa}\left[R-\left(\frac{\eta}{A\kappa}\right)^{\frac{1}{2}}\tanh\left(\frac{A\kappa}{\eta}\right)^{\frac{1}{2}}R\right],$$

where

ϕ = pressure gradient,
S = surface per gram,
A = constant,
κ = viscosity of water,
$R=d/2$,
η = viscosity of the film.

This gives for large canals the expression:

$$Q=2\phi R/SA\kappa$$

and for infinitely small canals:

$$Q=2\phi R^3/3S\eta.$$

Nevertheless, in spite of this theoretical difficulty, one can by using the experimental values of the flow for a given canal detect very accurately changes of state in monolayers. We have shown,[3] for example, that a liquid film of triolein exhibits at about 115A^2 a sharp change in the variation of the viscosity. In the same manner a fluid film of stearic acid on 0.001 N HCl gives changes at about 20.5 and 22A^2. Thus, from this point of view alone, the measurements of surface viscosity constitute already a very promising new method of investigation.

D. G. Dervichian
M. Joly

Laboratoire de Chimie physique,
Faculté des Sciences,
Paris, France,
March 16, 1938.

[1] Dervichian and Joly, Comptes rendus **204**, 1318 (1937). See also M. Joly, J. de phys. **8**, 471 (1937).
[2] Bresler and Talmud, Physik. Zeits. Sowjetunion **4**, 864 (1933).
[3] Dervichian and Joly, Comptes rendus **206**, 326 (1938).